The Plant Cell, Vol. 27: 857–873, March 2015, www.plantcell.org

ENHANCED DISEASE RESISTANCE4 Associates with CLATHRIN HEAVY CHAIN2 and Modulates Plant Immunity by Regulating Relocation of EDR1 in Arabidopsis

Guangheng Wu,[a,b] Simu Liu,[a,c] Yaofei Zhao,[a,c] Wei Wang,[a,c] Zhaosheng Kong,[b] and Dingzhong Tang[a,1]

[a] State Key Laboratory of Plant Cell and Chromosome Engineering, Institute of Genetics and Developmental Biology, Chinese Academy of Sciences, Beijing 100101, China

[b] State Key Laboratory of Plant Genomics, Institute of Microbiology, Chinese Academy of Sciences, Beijing 100101, China

[c] University of Chinese Academy of Sciences, Beijing 100049, China

Obligate biotrophs, such as the powdery mildew pathogens, deliver effectors to the host cell and obtain nutrients from the infection site. The interface between the plant host and the biotrophic pathogen thus represents a major battleground for plant-pathogen interactions. Increasing evidence shows that cellular trafficking plays an important role in plant immunity. Here, we report that *Arabidopsis thaliana* ENHANCED DISEASE RESISTANCE4 (EDR4) plays a negative role in resistance to powdery mildew and that the enhanced disease resistance in *edr4* mutants requires salicylic acid signaling. EDR4 mainly localizes to the plasma membrane and endosomal compartments. Genetic analyses show that *EDR4* and *EDR1* function in the same genetic pathway. EDR1 and EDR4 accumulate at the penetration site of powdery mildew infection, and EDR4 physically interacts with EDR1, recruiting EDR1 to the fungal penetration site. In addition, EDR4 interacts with CLATHRIN HEAVY CHAIN2 (CHC2), and *edr4* mutants show reduced endocytosis rates. Taken together, our data indicate that EDR4 associates with CHC2 and modulates plant immunity by regulating the relocation of EDR1 in Arabidopsis.

INTRODUCTION

Plants protect themselves against various pathogens through multiple layers of defense, including nonhost resistance and host resistance, which involve physical barriers and systems to detect nonself cues, via basal defense, and *RESISTANCE* (*R*) gene-mediated defenses (Schulze-Lefert and Panstruga, 2011; Nielsen and Thordal-Christensen, 2013). Detection of pathogen-associated molecular patterns (PAMPs) by pattern recognition receptors activates basal defense, which leads to PAMP-triggered immunity (PTI) (Boller and Felix, 2009). Specific recognition of pathogen effectors by R proteins leads to effector-triggered immunity (ETI) (Jones and Dangl, 2006). The defense responses associated with PTI and ETI may share signaling components and often include the activation of *PATHOGENESIS-RELATED* (*PR*) genes, mitogen-activated protein kinases (MAPKs), calcium-dependent protein kinases, and the hypersensitive response to restrict pathogen growth and spread (Tena et al., 2011).

Increasing evidence shows that vesicle trafficking plays an important role in the different layers of plant defense. For instance, forward genetic approaches identified *Arabidopsis thaliana PENETRATION1* (*PEN1*), *PEN2*, and *PEN3*, which play positive roles in nonhost resistance; loss of function of each *PEN* results in defects in penetration resistance to the nonadapted powdery mildew pathogen *Blumeria graminis* f sp *hordei* (Collins et al., 2003; Lipka et al., 2005; Stein et al., 2006; Underwood and Somerville, 2008). In addition to penetration resistance, vesicle trafficking also plays important roles in PTI and ETI (Robatzek, 2014). For instance, the Arabidopsis PAMP receptor FLAGELLIN SENSING2 (FLS2), a well-characterized pattern recognition receptor, recognizes flagellin, a subunit of the bacterial flagellum (Zipfel et al., 2004), and activates the downstream signaling pathway (Veronese et al., 2006; Chinchilla et al., 2007; Lu et al., 2010; Shi et al., 2013). FLS2 localizes to the plasma membrane, and after activation by flagellin, FLS2 is internalized into the cell (Robatzek et al., 2006). Blocking flagellin-activated FLS2 endocytosis alters defense against bacterial pathogens (Robatzek et al., 2006; Spallek et al., 2013). FLS2 endocytosis requires ENDOSOMAL SORTING COMPLEX REQUIRED FOR TRANSPORT-I (Spallek et al., 2013). In addition, the ARF-GEF family protein MIN7, a key component of the vesicle-trafficking machinery, is required for PTI and ETI to *Pto* DC3000 infection in Arabidopsis. Also, the bacterial effector HopM1 targets MIN7 for the suppression of host resistance (Nomura et al., 2006, 2011).

Vesicle trafficking plays important roles, including in disease resistance against filamentous organisms (e.g., fungi and oomycetes, such as powdery mildew) (Yi and Valent, 2013). Powdery mildew pathogens are common and widespread obligate biotrophs that infect large numbers of plants. When a powdery mildew fungal spore infects a plant, the fungus produces a germ tube and appressorium that directly penetrate into epidermal cells and then develops a haustorium (Koh et al., 2005). The haustorium differentiates from the penetration hypha and plays important roles in transporting effectors into the cell and acquiring nutrition from the host (Panstruga and Dodds, 2009; Hückelhoven and

[1] Address correspondence to dztang@genetics.ac.cn.
The author responsible for distribution of materials integral to the findings presented in this article in accordance with the policy described in the Instructions for Authors (www.plantcell.org) is: Dingzhong Tang (dztang@genetics.ac.cn).
www.plantcell.org/cgi/doi/10.1105/tpc.114.134668

Panstruga, 2011). Work in Arabidopsis has identified, in addition to *PEN1*, *PEN2*, and *PEN3*, a number of genes that function in powdery mildew resistance. For instance, *ENHANCED DISEASE RESISTANCE1* (*EDR1*) encodes a Raf-like MAPK kinase kinase that negatively regulates salicylic acid (SA)-inducible defense responses (Frye et al., 2001). The N-terminal regulatory domain of EDR1 physically interacts with MKK4 and MKK5 and negatively affects MKK4/MKK5 and MPK3/6 protein levels. Also, mutations in *MPK3*, *MKK4*, or *MKK5* can suppress *edr1*-mediated resistance, indicating that EDR1 fine-tunes plant innate immunity by negatively regulating the MAPK cascade (Zhao et al., 2014). *KEEP ON GOING* (*KEG*) encodes a protein containing a RING E3 ligase domain and a kinase domain, and a specific missense mutation in *KEG* suppresses *edr1*-associated phenotypes. KEG interacts with EDR1 and recruits it to the *trans*-Golgi network/early endosome (TGN/EE) vesicles (Wawrzynska et al., 2008; Gu and Innes, 2011). KEG regulates endomembrane protein trafficking and is degraded specifically in cells infected by powdery mildew (Gu and Innes, 2012). Recent work showed that EDR1 also interacts with ARABIDOPSIS TOXICOS EN LEVADURA1 (ATL1), an E3 ubiquitin ligase that positively regulates resistance and cell death. Overexpression of ATL1 causes cell death in Arabidopsis and *Nicotiana benthamiana*, and the cell death induced by ATL1 can be suppressed by EDR1. In addition, knockdown of *ATL1* expression suppressed *edr1*-mediated powdery mildew resistance, indicating that ATL1 is a potential substrate of EDR1 (Serrano et al., 2014). *EDR2* encodes a protein that contains a pleckstrin homology domain and a steroidogenic acute regulatory protein-related lipid-transfer domain (Tang et al., 2005; Vorwerk et al., 2007). EDR2 mainly localizes to the endoplasmic reticulum (ER) and also localizes to the plasma membrane and endosomes (Vorwerk et al., 2007). Genetic analyses showed that mutations in the transcription factor SR1, the 26S proteasome subunit RPN1a, or the receptor-like cytoplasmic kinase BSK1 can suppress *edr1*- and *edr2*-mediated resistance (Nie et al., 2012; Yao et al., 2012; Shi et al., 2013). *EDR3* encodes DYNAMIN-RELATED-PROTEIN 1E, which is thought to be involved in membrane tubulation, a process essential for vesicle scission (Hong et al., 2003; Tang et al., 2006). Although vesicle trafficking is implicated in powdery mildew resistance mediated by *edr1* and *edr3*, the mechanism by which vesicle trafficking affects resistance remains unclear.

The plasma membrane is a source and a sink for the endocytic and exocytic vesicle-trafficking pathways. Clathrin-mediated endocytosis (CME) is the major route of endocytosis (Dhonukshe et al., 2007). CME initiates at the plasma membrane, where cargo and coat machinery are recruited into clathrin-coated pits (Chen et al., 2011). GTPase dynamins scissor off the clathrin-coated pits after maturation to form clathrin-coated vesicles, which then target to and fuse with the early endosome. In the early endosome, cargo is differentially sorted for recycling back to the plasma membrane or to the vacuole for degradation (McMahon and Boucrot, 2011). CME complex components include clathrin, adaptor protein complexes, and accessory adaptor proteins, which bind directly to cargo or cargo receptors. Various accessory adaptor proteins can transport many different cargoes, making CME very versatile (McMahon and Boucrot, 2011). Clathrin subunits form triskelion, composed of three clathrin heavy chains and three clathrin light chains that self-polymerize (Chen et al., 2011; McMahon and Boucrot, 2011). The Arabidopsis genome has two clathrin heavy chain and three clathrin light chain genes (Chen et al., 2011). Genetic analyses show that those genes are critical for endocytosis and other clathrin-mediated pathways; for instance, *clathrin heavy chain2* (*chc2*) mutants show defects in endocytosis and the internalization of auxin transporters (Kitakura et al., 2011). Recent work showed that SA, which usually associates with biotrophic pathogen defenses, also interferes with clathrin-mediated endocytic trafficking (Du et al., 2013). Although many components of CME remain to be identified, the recent identification and characterization of CME adaptors shed new light on how CME functions in plants (Gadeyne et al., 2014).

To identify components involved in powdery mildew resistance, we screened Arabidopsis mutants for enhanced disease resistance to the powdery mildew pathogen *Golovinomyces cichoracearum* (Tang et al., 2005). Here, we show that the loss-of-function *edr4* mutant displays enhanced disease resistance to powdery mildew. EDR4 interacts with CHC2, one of the heavy chains of clathrin, and the *edr4* mutants show reduced endocytosis rates. In addition, EDR4 interacts with EDR1 and recruits EDR1 to the site of fungal penetration, indicating that EDR4 plays an important role in plant immunity. We propose that EDR4 might modulate plant immunity by recruiting and transporting EDR1 to its destination.

RESULTS

The *edr4-1* Mutants Display Enhanced Disease Resistance to *G. cichoracearum*

To study the molecular interactions between Arabidopsis and powdery mildew, we previously screened ethyl methanesulfonate-mutagenized Arabidopsis Columbia-0 (Col-0) plants for enhanced disease resistance to *G. cichoracearum* (Tang et al., 2005). Among three mutants identified in this screen, *edr2* and *edr3* have been described (Tang et al., 2005, 2006); here, we describe our characterization of the *edr4-1* mutant.

The *edr4-1* mutants did not show any growth defects under short-day conditions; however, they displayed mild, hypersensitive response-like lesions under long-day conditions at late growth stages (Supplemental Figure 1). To characterize powdery mildew resistance in *edr4-1*, we infected 4-week-old plants with *G. cichoracearum* UCSC1 under short-day conditions. The wild-type plants were susceptible and supported abundant conidiophores on their leaves at 8 d after inoculation (DAI). However, the *edr4-1* mutants showed fewer conidiophores and massive necrotic lesions on the leaves at 8 DAI (Figures 1A to 1C). To further monitor fungal reproduction, we counted the conidiophores per colony in wild-type and *edr4-1* plants. As shown in Figure 1D, significantly fewer conidiophores were produced on *edr4-1* leaves than on wild-type leaves at 6 DAI, indicating that the growth of powdery mildew fungus was inhibited in the *edr4-1* mutant.

Activation of plant defenses often involves the production of H_2O_2 and the deposition of callose. To examine whether *edr4-1* mutants accumulate more H_2O_2 than the wild type after infection, we used 3,3′-diaminobenzidine hydrochloride (DAB) to stain infected leaves at 2 DAI with *G. cichoracearum*. The *edr4-1* mutants showed more pronounced H_2O_2 accumulation in the infection site than did wild-type plants (Figure 1E; Supplemental

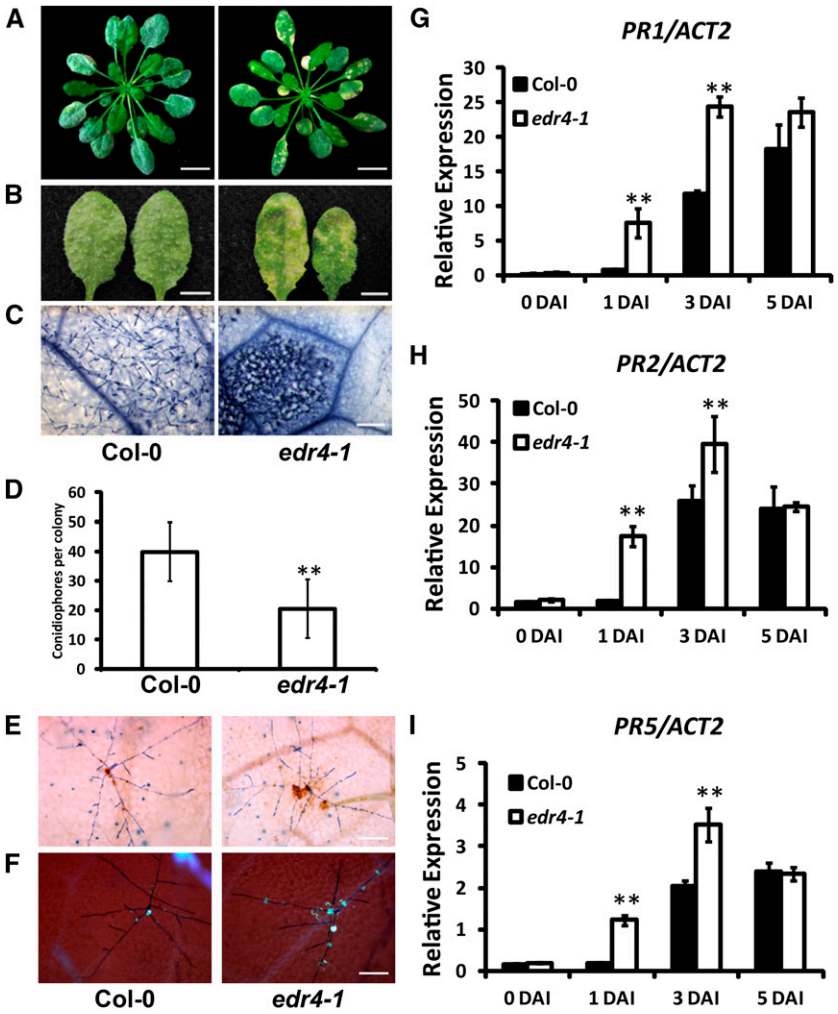

Figure 1. The *edr4-1* Mutant Exhibited Enhanced Disease Resistance to *G. cichoracearum*.

(A) Four-week-old wild-type and *edr4-1* plants inoculated with *G. cichoracearum* UCSC1. The photographs were taken at 8 DAI. Bars = 1 cm.
(B) Representative leaves removed from 4-week-old wild-type and *edr4-1* plants inoculated with *G. cichoracearum*. The photographs were taken at 8 DAI. Bars = 0.5 cm.
(C) Trypan blue staining of the leaves shown in **(B)** to visualize fungal structures and plant cell death. Bar = 100 μm.
(D) Quantitative analysis of conidiophore formation on 4-week-old wild-type and *edr4-1* plants at 6 DAI. The bars represent means and SD in one experiment (n = 20). The experiment was repeated three times with similar results. The asterisks indicate a statistically significant difference from the wild type ($P < 0.01$, Student's t test).
(E) Trypan blue-DAB staining of 4-week-old wild-type and *edr4-1* plants at 2 DAI with *G. cichoracearum*. Brown staining shows the accumulation of H_2O_2. Bar = 100 μm.
(F) Aniline blue staining of 4-week-old wild-type and *edr4-1* plants at 2 DAI with *G. cichoracearum* to visualize callose deposition (blue dots). Bar = 100 μm.
(G) to **(I)** Four-week-old wild-type and *edr4-1* plants were inoculated with *G. cichoracearum*. Relative transcript levels of *PR1*, *PR2*, and *PR5* were examined at various time points using real-time PCR with *ACT2* as an internal control. Bars represent means and SD of values obtained from three experiments. Asterisks indicate significant differences from the wild type ($P < 0.01$, Student's t test).

Figures 2A and 2B). To monitor callose deposition in wild-type and *edr4-1* mutant plants, we performed aniline blue staining on the infected leaves at 2 DAI and found that the *edr4-1* mutants showed more callose deposition at the infection site than the wild type (Figure 1F; Supplemental Figures 2C and 2D).

To investigate whether the *edr4-1* mutation affects the expression of defense-related genes, we examined the transcript levels of *PR1*, *PR2*, and *PR5* in wild-type and *edr4-1* mutant plants at different time points after *G. cichoracearum* infection using real-time PCR. Both the wild type and *edr4-1* showed relatively low accumulation of *PR1*, *PR2*, and *PR5* transcripts before infection. The transcript levels of *PR* genes increased after inoculation in both the wild type and *edr4-1*, but significantly more transcripts of *PR* genes accumulated in *edr4-1* plants than in wild-type plants at 1 and 3 DAI (Figures 1G to 1I). These observations indicate that the *edr4-1* mutants induced

the defense response more rapidly than the wild-type plants did.

The Enhanced Disease Resistance in *edr4-1* Mutants Depends on SA Signaling

SA, jasmonic acid (JA), and ethylene signaling pathways play important roles in plant defense responses. To examine whether those pathways affect *edr4-1*-mediated resistance, we constructed double mutants and assessed whether mutations in those pathways alter powdery mildew resistance in *edr4-1*. The *npr1* mutation, which disrupts SA perception, and the *pad4*, *eds1*, *eds5*, and *sid2* mutations, which reduce levels of pathogen-induced SA, suppressed *edr4-1*-mediated enhanced resistance to powdery mildew and mildew-induced cell death (Figure 2A; Supplemental Figure 3). By contrast, mutations in *EIN2* or *COI1* blocked the ethylene response or the JA response, respectively, and did not affect *edr4-1* resistance and mildew-induced cell death (Figure 2A; Supplemental Figure 3). These data indicate that *edr4-1*-mediated resistance and mildew-induced cell death phenotypes are SA-dependent but ethylene- and JA-independent.

To further assess the role of SA in *edr4-1*-mediated resistance, we measured SA levels in the wild type and *edr4-1* before and after infection with *G. cichoracearum*. In the absence of pathogen, the *edr4-1* mutants and wild-type plants had similar levels of free and total SA; by contrast, at 3 DAI, SA accumulated at much higher levels in *edr4-1* than in the wild type (Figure 2B). These data indicate that higher SA levels in *edr4-1* mutants cause the enhanced disease resistance and mildew-induced cell death.

EDR4 Encodes a Protein of Unknown Function

The *edr4-1* mutation was identified by standard map-based cloning (Supplemental Figure 4A). A C-to-T transition at nucleotide 1213 in At5g05190 was found in *edr4-1*, and this transition causes an early stop (Q405STOP) in the predicted protein sequence (Supplemental Figure 4A). To confirm that At5g05190 is *EDR4*, a genomic clone of At5g05190 was transformed into *edr4-1* plants. Among 25 transgenic plants obtained, 22 displayed the wild-type, susceptible phenotype at 8 DAI when infected with *G. cichoracearum*, indicating that the At5g05190 genomic clone complemented the *edr4-1* phenotype (Supplemental Figures 4B and

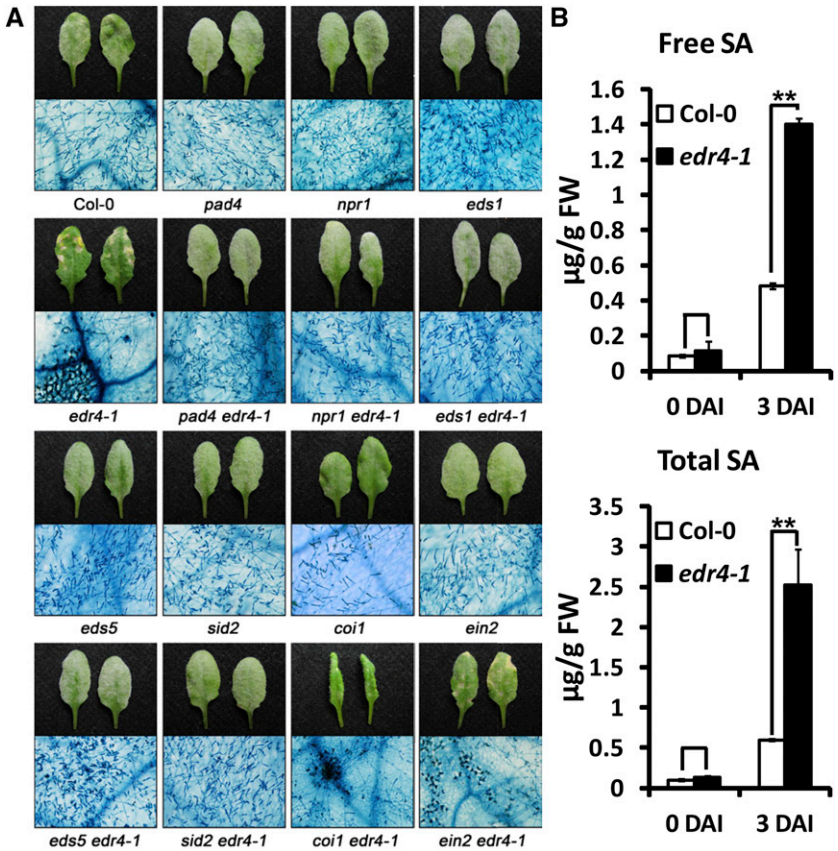

Figure 2. The Enhanced Disease Resistance Mediated by *edr4-1* Requires the SA Signaling Pathway.

(A) Four-week-old plants were inoculated with *G. cichoracearum*, and representative leaves were removed and photographed (top panels) or stained with trypan blue (bottom panels) at 8 DAI. The *edr4-1*-mediated resistance is suppressed by *pad4*, *npr1*, *eds1*, *eds5*, and *sid2* but not by *coi1* or *ein2*. Bar = 200 μm.
(B) Free and total SA was extracted from 4-week-old wild-type and *edr4-1* leaves at 0 and 3 DAI, then the SA levels were determined by HPLC. The bars represent means and SD ($n = 6$). The experiment was repeated three times with similar results. The asterisks indicate statistically significant differences from the wild type ($P < 0.01$, Student's t test). FW, fresh weight.

4C). As an additional confirmation, we also examined the phenotypes of two T-DNA insertion lines of At5g05190, SALK_048465 (*edr4-2*) and SALK_009370 (*edr4-3*) (Supplemental Figure 4A). No full-length transcript of At5g05190 could be detected in *edr4-1* or in these two lines, indicating that the expression of *EDR4* is disrupted in these three mutant lines (Supplemental Figure 4D). These two mutants showed enhanced disease resistance and mildew-induced cell death upon powdery mildew infection at 8 DAI, which was very similar to the phenotype of *edr4-1* (Supplemental Figures 4B and 4C). Taken together, these data indicate that At5g05190 is the gene responsible for the *edr4-1* phenotypes; therefore, we designate At5g05190 as *EDR4*.

EDR4 encodes a protein of 615 amino acids with no assigned function, and no clear EDR4 homolog could be identified in the Arabidopsis genome. A search for motifs in the primary sequence of EDR4, using the Eukaryotic Linear Motif server (http://elm.eu.org/) (Puntervoll et al., 2003), identified three types of structural elements in EDR4: a coiled-coil (CC) domain, four low-complexity regions (LCR), and a Duf3133 domain of unknown function (Supplemental Figure 4E). The CC domain and LCRs often function as protein interaction domains for a wide variety of proteins (Burkhard et al., 2001; Lee et al., 2011).

EDR4 Mainly Localizes at the Plasma Membrane and Endosomal Compartments

To investigate the subcellular localization of EDR4, we made a fusion of EDR4 to Green Fluorescent Protein (GFP), expressed it from the *pEDR4-EDR4-eGFP* construct (*EDR4-GFP*), and transformed it into *edr4-1* mutant plants. EDR4-GFP was expressed as a full-length protein and complemented the *edr4-1* phenotypes, indicating that EDR4-GFP was functional (Supplemental Figure 5). A representative homozygous *edr4-1 EDR4-GFP* transgenic line was chosen to examine EDR4 localization. In root tip cells of 5-d-old seedlings, time-lapse analysis revealed that EDR4-GFP displayed dynamic intracellular movement, which partially overlapped with FM4-64 (Supplemental Figure 6A and Supplemental Movie 1). EDR4-GFP appears to localize on the plasma membrane and on dot-like intracellular structures in the cytosol. To determine the subcellular localization of EDR4, we assessed the colocalization of EDR4-GFP with several organelle markers, including mCherry-SYP61 (TGN/EE), ARA6-mCherry (late endosome), SYP32-mCherry (*cis*-Golgi), and HDEL-mCherry (ER) (Nelson et al., 2007; Geldner et al., 2009; Gu and Innes, 2011, 2012; Sauer et al., 2013), and examined EDR4-GFP in root tips of transgenic plants. Microscopy and quantification analysis showed that a large portion of EDR4-GFP protein overlapped with the TGN/EE marker SYP61, the late endosome marker ARA6, and the *cis*-Golgi marker SYP32, but a smaller portion of EDR4-GFP overlapped with the ER marker HDEL (Figures 3A to 3E). Taken together, these data indicate that EDR4 mainly localizes at the plasma membrane and in endosomal compartments and displays dynamic movement in cells.

EDR4 Accumulates at the Penetration Site of Fungal Infection

We further examined the subcellular localization of EDR4 in epidermal cells after *G. cichoracearum* infection using the *EDR4-GFP* transgenic line. The GFP signal was observed in epidermal cells in uninfected leaves (Figure 4A) and also showed intracellular movement (Supplemental Figure 6B and Supplemental Movie 2). At 48 h after inoculation (HAI) with *G. cichoracearum*, EDR4-GFP accumulated under the penetration peg at the infection site in epidermal cells (Figure 4B), but overall, the EDR4-GFP protein levels decreased at 72 HAI with *G. cichoracearum* (Figure 4C). To further confirm the accumulation of EDR4-GFP at the site of infection, we also examined EDR4-GFP localization at 24 HAI, with the *cis*-Golgi-localized protein *N*-acetylglucosaminyltransferase I (NAG) fused to GFP (Essl et al., 1999) as a control. Fungal structures were labeled with propidium iodide. We found that EDR4-GFP accumulated at penetration sites at 24 HAI (Figures 4D and 4E), while there was no obvious difference in the subcellular localization of NAG-GFP before and after inoculation (Supplemental Figure 7). To determine whether EDR4 accumulates at the plasma membrane or papillae at the penetration site after infection, we used plasmolysis of infected leaves at 24 HAI. As shown in Supplemental Figure 8A, EDR4-GFP accumulated in the plasma membrane but not in papillae.

EDR1, *EDR4*, and *KEG* Act in the Same Genetic Pathway

To further characterize the *edr4-1* mutant, we crossed *edr4-1* with *edr1* and *edr2*, two well-characterized powdery mildew resistance mutants, and examined the phenotypes of the double mutants. The *edr2 edr4-1* mutant showed more cell death and fewer fungal spores than the *edr2* and *edr4-1* single mutants, indicating that the *edr2* mutation enhanced the *edr4-1* phenotype. However, the *edr1*, *edr4-1*, and *edr1 edr4-1* mutants showed no significant differences in growth of fungal spores (Supplemental Figure 9). A missense mutation in *KEG* (*keg-4*) suppressed the *edr1* phenotype (Wawrzynska et al., 2008). To further examine the relationship between EDR1 and EDR4, we crossed *edr1*, *edr4-1*, and *edr1 edr4-1* with *keg-4* and generated double and triple mutants. The *keg-4* mutation suppressed the enhanced disease resistance of *edr4* and *edr1 edr4-1* mutants (Figures 5A and 5B), indicating that *edr4*-mediated resistance also requires *KEG*. Previous work showed that *keg-4* suppresses *edr1*-mediated resistance, but not *edr2*-mediated resistance, indicating that *keg-4* specifically suppresses *edr1* (Yao et al., 2012). The observations that *keg-4* suppressed *edr4-1* and *edr1 edr4-1*, and that *edr1*, *edr4-1*, and *edr1 edr4-1* displayed similar levels of resistance, suggest that *EDR1*, *EDR4*, and *KEG* act in the same genetic pathway. Consistent with this notion, MPK3 and MPK6 kinase activation increased in *edr4-1* mutants upon infection by *G. cichoracearum*, and *mpk3*, *mkk4*, and *mkk5* mutations also suppressed powdery mildew resistance in *edr4-1* (Supplemental Figure 10), similar to the *edr1* mutant (Zhao et al., 2014).

EDR4 Interacts with EDR1

Since *edr1* and *edr4-1* displayed similar powdery mildew resistance, and *EDR1*, *EDR4*, and *KEG* may act in the same genetic pathway, we hypothesized that EDR4 may associate with EDR1 to modulate plant immunity. To test this hypothesis, we performed yeast two-hybrid assays to examine whether EDR4 interacts with EDR1 and KEG. EDR4 could interact with the N-terminal domain

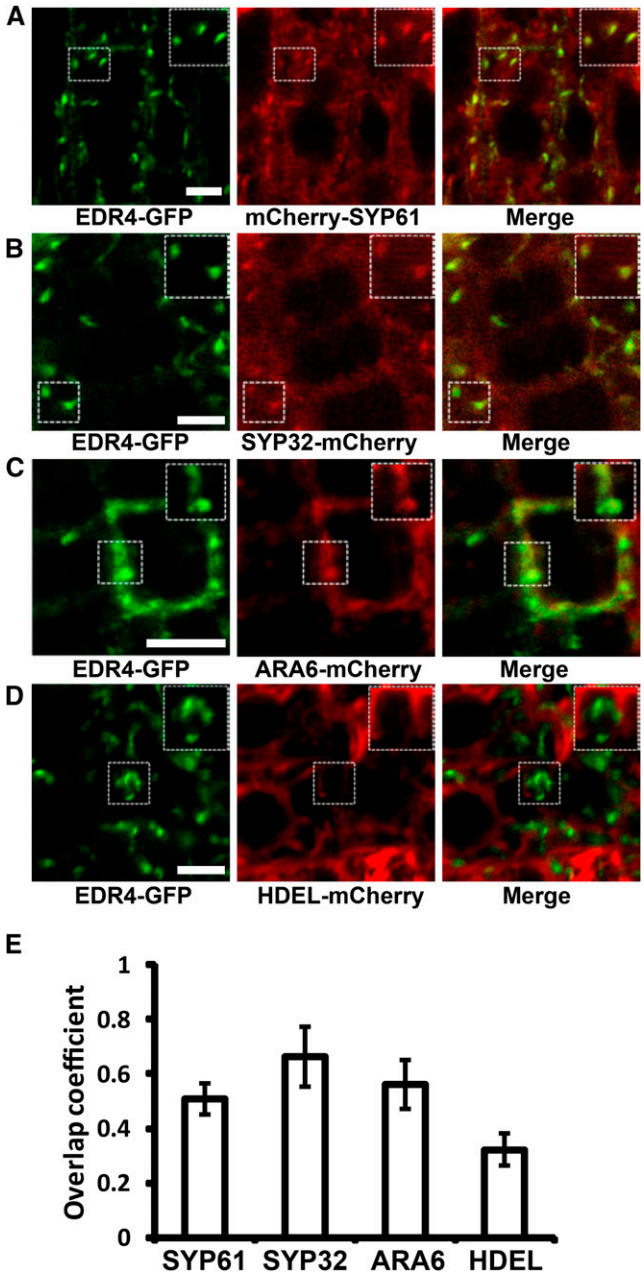

Figure 3. EDR4 Localizes to the Plasma Membrane, TGN/EE, and *cis*-Golgi.

(A) to **(D)** The root tip cells of 5-d-old seedlings that expressed EDR4-GFP and the indicated subcellular markers were imaged using confocal microscopy, and single optical sections are shown. Enlarged images of the boxed areas are shown at top right. The *mCherry-SYP61* **(A)** and *ARA6-mCherry* **(C)** constructs were introduced into the EDR4-GFP plants by transformation, while *SYP32-mCherry* **(B)** and *HDEL-mCherry* **(D)** were introduced into the EDR4-GFP plants by genetic crosses. Bars = 5 μm.
(E) Quantitative analysis of the overlap of EDR4-GFP with the indicated organelle markers. The bars show Mander's overlap coefficient (Herda et al., 2012), indicating a level of colocalization between EDR4-GFP and the organelle marker. Two independent experiments with 20 to 35 cells for each subcellular marker were evaluated.

(amino acids 1 to 657) of EDR1 and full-length EDR1 but not with the C-terminal domain of EDR1 (amino acids 658 to 933) or with KEG (Figure 6A; Supplemental Figure 11). To determine which domain of EDR4 is responsible for the interaction with EDR1, we conducted a deletion analysis of EDR4 and examined the interactions of the deleted variants by yeast two-hybrid assays. As shown in Figure 6A, a variant of EDR4 with only the CC domain (amino acids 1 to 149) could interact with EDR1, while the LCR, Duf3133 domain, or CC domain deletion form of EDR4 could not interact with EDR1. These data indicate that the CC domain of EDR4 is necessary and sufficient for interaction with EDR1.

To further confirm the interactions of EDR1 and EDR4, we performed bimolecular fluorescence complementation (BiFC) by fusing EDR1, EDR4, and EDR4 deletion forms or KEG to the N- or C-terminal fragment of Yellow Fluorescent Protein (YFP) and transiently expressing those constructs in *N. benthamiana* leaves. We observed reconstituted YFP fluorescence in leaves cotransformed with 35S-driven YN-EDR1 and YC-KEG, as well as YN-EDR1 and YC-EDR4 or the YC-CC-EDR4 domain, but not in leaves cotransformed with YN-KEG and YC-EDR4 or other YC-EDR4 deletions (Figure 6B; Supplemental Figure 12), indicating that the EDR4 CC domain interacts with EDR1 in *N. benthamiana*, consistent with the results of the yeast two-hybrid assays.

To validate the interaction of EDR4 and EDR1, we also performed coimmunoprecipitation (Co-IP) assays in stable transgenic Arabidopsis plants. We crossed *EDR4-GFP* plants with plants expressing *EDR1-FLAG* driven by the native *EDR1* promoter and used the F2 plants that express both EDR4-GFP and EDR1-FLAG in Co-IP assays, with plants that expressed both EDR1-FLAG and GFP as a negative control. We extracted total protein and immunoprecipitated EDR1 using anti-FLAG antibody and then detected the presence or absence of EDR4 with anti-GFP antibody. EDR4 was detected only in the precipitates of leaves that express EDR1-FLAG and EDR4-GFP but not in the negative control plants (Figure 6C), indicating that EDR4 interacts with EDR1 in Arabidopsis. Taken together, these observations indicate that EDR4 interacts with EDR1.

Since EDR1 interacts with EDR4, we then examined whether EDR4 colocalizes with EDR1. We first transiently expressed EDR4-GFP and EDR1-mCherry in *N. benthamiana* leaves. EDR1 appears to colocalize with EDR4 in the plasma membrane and endosomal compartments (Supplemental Figures 13A and 13B). We then examined transgenic plants that coexpressed EDR4-GFP and EDR1-mCherry. Similarly, EDR4-GFP and EDR1-mCherry colocalized in endosomal compartments in root cells (Supplemental Figure 13C).

EDR4 Recruits EDR1 to Powdery Mildew Infection Sites on the Plasma Membrane

Since EDR1 interacts with EDR4, we next examined whether EDR1 and EDR4 have similar localization patterns. EDR1 also shows dynamic intracellular movement (Supplemental Figure 6C and Supplemental Movie 3). As EDR4 accumulated at powdery mildew infection sites, we then examined whether EDR1 also accumulates at infection sites and whether the *edr4-1* mutation affects this localization. We thus crossed the *EDR1-GFP* transgenic plant with the *edr4-1* mutant to generate *edr4-1 EDR1-GFP* plants. We did not observe an obvious difference in EDR1-GFP localization in

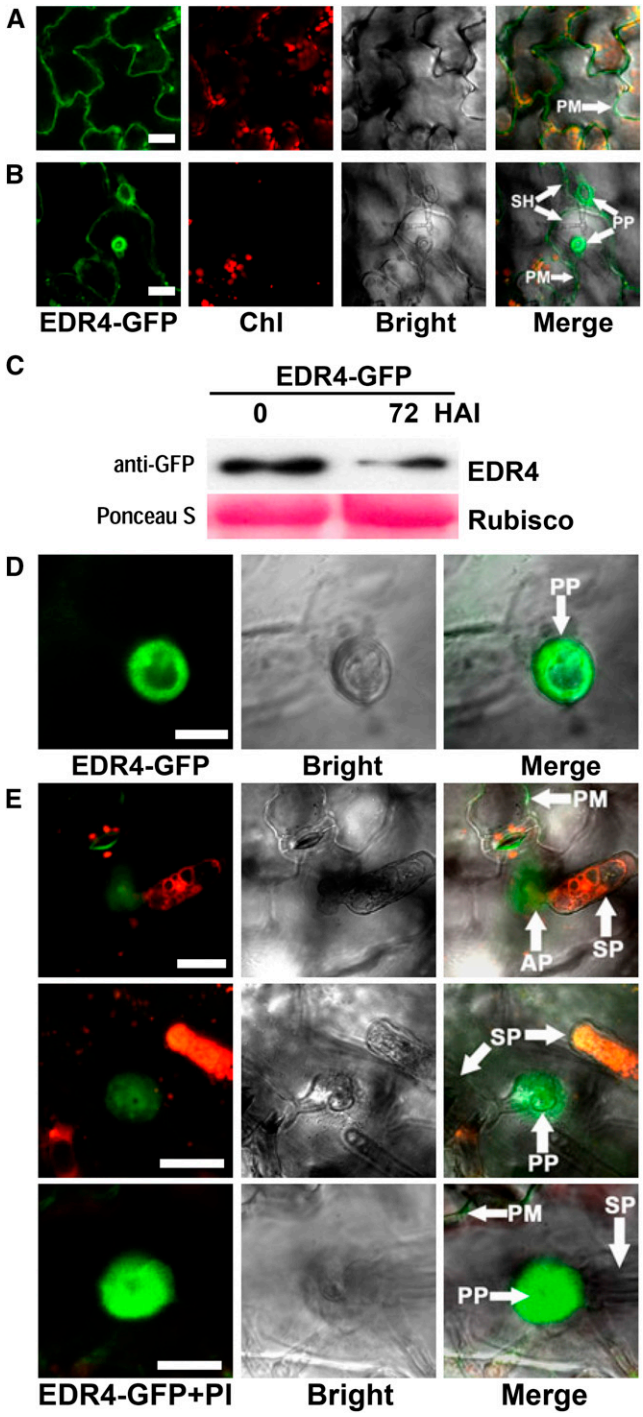

Figure 4. EDR4-GFP Accumulates at the Powdery Mildew Penetration Site in Epidermal Cells.

(A) EDR4-GFP localization in epidermal cells of uninfected leaves. Bar = 25 μm.

(B) EDR4-GFP accumulates under the penetration peg of the secondary hyphal infection site in epidermal cells at 48 HAI with *G. cichoracearum*. Bar = 25 μm.

(C) Four-week-old transgenic EDR4-GFP plants were infected with *G. cichoracearum*. Immunoblotting was performed using an anti-GFP antibody. Ponceau S staining of Rubisco is shown as a loading control. The experiment was repeated at least three times with similar results.

(D) and **(E)** Accumulation of EDR4-GFP around the penetration peg of the appressorium at 24 HAI with *G. cichoracearum*, shown in different views. Leaves in **(E)** were stained with propidium iodide (PI) to visualize the fungal structures, which appear red. Bar in **(D)** = 10 μm; bars in **(E)** = 20 μm.

AP, appressoria; Chl, chloroplast; PM, plasma membrane; PP, penetration peg; SH, secondary hyphae; SP, spores.

wild-type and *edr4-1* backgrounds in the absence of powdery mildew pathogen (Supplemental Figure 14A). Upon infection, EDR1-GFP also accumulated at the infection site at 24 HAI in wild type leaves; however, EDR1-GFP accumulated at much lower levels at infection sites in *edr4-1* leaves (Figures 7A and 7B). To quantify the level of accumulation of EDR1-GFP, we calculated the frequency of focal accumulations of EDR1-GFP at infection sites in wild-type and *edr4-1* plants according to the previously described method (Underwood and Somerville, 2013). As shown in Figure 7C, the frequency of focal accumulations of EDR1-GFP in *edr4-1* mutants was much lower than in the wild type, indicating that the *edr4-1* mutation compromised the accumulation of EDR1-GFP at the fungal infection site. Similar to EDR4-GFP, plasmolysis analysis showed that EDR1-GFP also accumulated at the plasma membrane, not in papillae, after infection with *G. cichoracearum* (Supplemental Figure 8B). Taken together, our data suggested that EDR1 moves to the plasma membrane around powdery mildew infection sites and that EDR4 plays an important role in EDR1 relocation.

As the CC domain of EDR4 is necessary for interaction with EDR1, we examined whether EDR1 localization was affected in the EDR4 CC domain deletion background. We made an EDR4-CC-domain deletion-FLAG construct and transformed it alone or with the *pEDR1-EDR1-GFP* construct into *edr4-2*. The EDR4-CC-domain deletion-FLAG construct did not complement the *edr4-2* phenotype, indicating that EDR4 function requires the CC domain (Supplemental Figure 15). We also compared EDR1 localization in wild-type, *edr4-2*, and *edr4-2* EDR4-CC-domain deletion plants after powdery mildew infection. The localization of EDR1-GFP in the *edr4-2* and *edr4-2* EDR4-CC-domain deletion background was similar, as both show defects in focal accumulation to the site of mildew infection (Supplemental Figure 16), indicating that the EDR4-CC-domain deletion construct could not function as the full-length EDR4 protein. To examine whether *edr1* affected EDR4 localization, we examined EDR4-GFP localization in wild-type and *edr1* plants after powdery mildew infection at 24 HAI. EDR4-GFP accumulated at the infection site in wild-type and *edr1* plants, and no significant difference was observed between the wild type and *edr1*, indicating that *edr1* did not affect the localization of EDR4 (Supplemental Figure 17).

To examine whether powdery mildew triggers continuous accumulation of EDR1 and EDR4, we performed fluorescence recovery after photobleaching (FRAP) (Bhat et al., 2005) of *EDR1-GFP* and *EDR4-GFP* leaves at *G. cichoracearum* penetration sites and distal membrane sites. At the penetration site, the EDR1-GFP signal recovered to less than 40% in 60 min, compared with before bleaching, and EDR4-GFP displayed a similar pattern, recovering to less than 20% in 60 min (Supplemental Figures 18A and 18C). By contrast, at a distal membrane site, the EDR1-GFP and EDR4-GFP signals showed rapid recovery (within 15 min) after bleaching

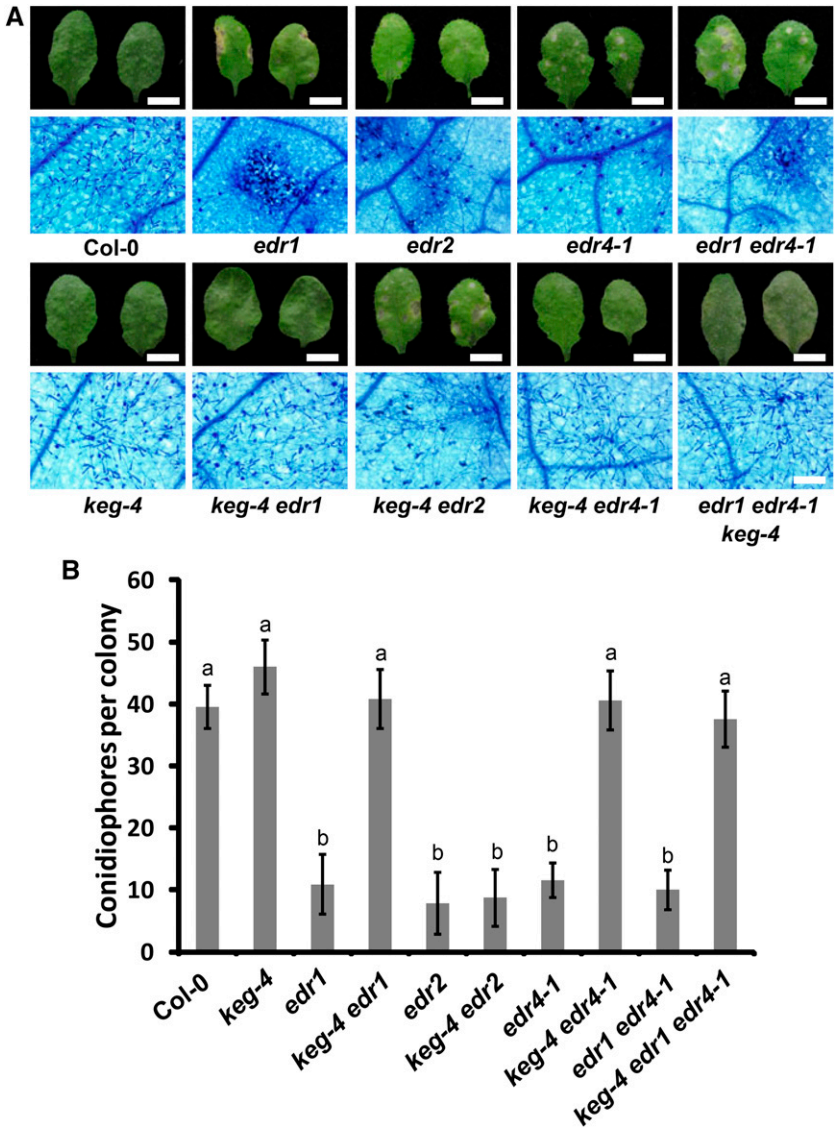

Figure 5. The *edr1* Suppressor *keg-4* Suppresses *edr4-1*-Mediated Powdery Mildew Resistance.

(A) Photograph and trypan blue staining of representative leaves removed from 4-week-old plants at 8 DAI with *G. cichoracearum*. Bars in top panels = 0.5 cm; bar in bottom panels = 100 μm.

(B) Quantitative analysis of conidiophore formation on infected plants at 6 DAI. The bars represent means and SD (n = 20). The samples are labeled with different letters to indicate statistically significant differences ($P < 0.01$, one-way ANOVA). The experiments were repeated three times with similar results.

(Supplemental Figures 18B and 18D). These data suggested that EDR1 and EDR4 proteins were not continuously delivered to penetration sites but were delivered one time and retained at these sites. These results are comparable to previous findings that focal accumulations of PEN1 and PEN3 after *B. graminis* f sp *hordei* infection result from single delivery events rather than continuous delivery (Bhat et al., 2005; Underwood and Somerville, 2013).

EDR4 Interacts with CHC2, and *edr4* Shows Reduced Endocytosis Rates

The Arabidopsis Interactome Mapping Consortium (2011) reported that EDR4 could interact with CHC2, a major component of clathrin-coated vesicles in CME and clathrin-mediated pathways in yeast two-hybrid assays. To confirm the interactions between CHC2 and EDR4 in planta, we performed BiFC assays using *N. benthamiana*. As shown in Figure 8A, we observed YFP signal in leaves coexpressing CHC2 and full-length EDR4, the EDR4 CC domain, or the EDR4 LCR domain but not the EDR4 Duf3133 domain, confirming that EDR4 interacts with CHC2 and that the CC and LCR domains may be responsible for this interaction. The interaction between EDR4 and CHC2 suggested that EDR4 could function in clathrin-mediated pathways. To further confirm the interaction between EDR4 and CHC2, we performed Co-IP assays in stable transgenic Arabidopsis plants. We crossed EDR4-GFP plants with plants expressing MYC-N-CHC2 driven by

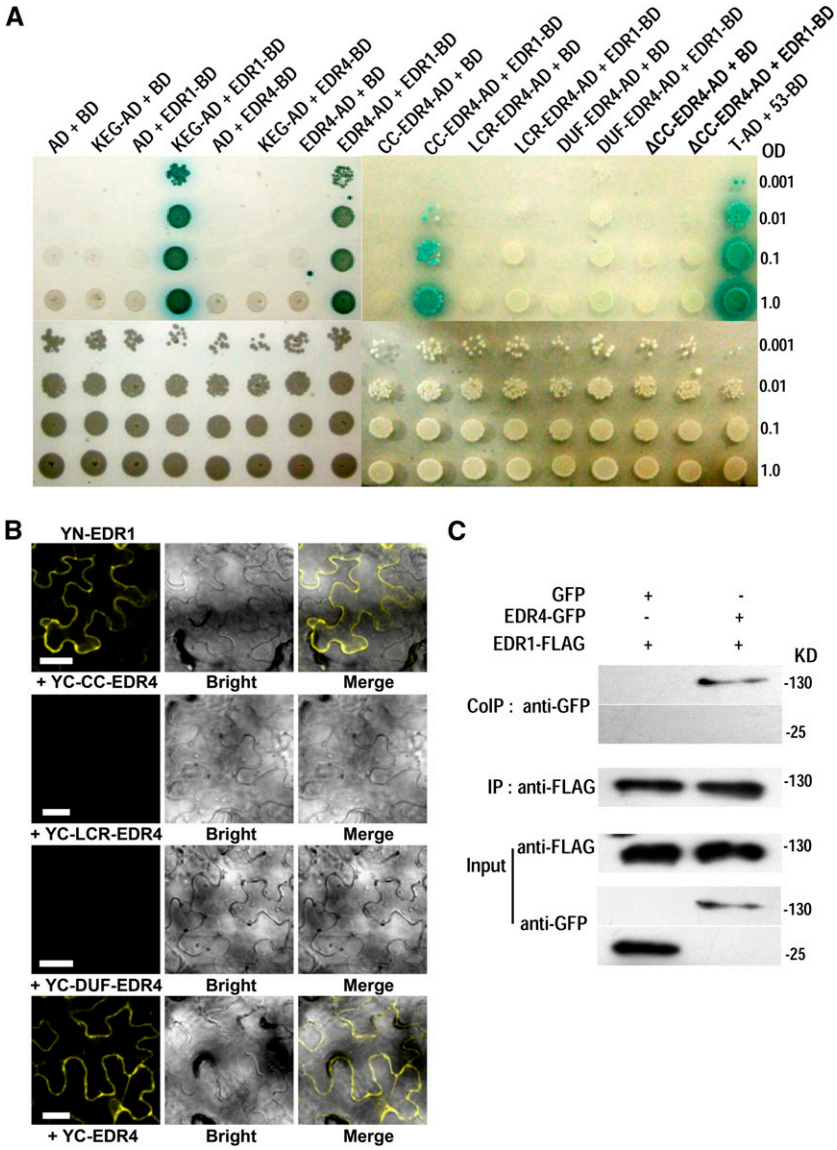

Figure 6. EDR4 Interacts with EDR1.

(A) EDR4 interacts with EDR1 in yeast two-hybrid assays. Yeast cells containing the indicated plasmids were serially diluted from OD_{600} = 1 and spotted on control medium and on selective medium supplemented with 25 mM 3-amino-1,2,4-triazole and 40 μg/mL X-α-Gal. AD and BD represent pGADT7 and pGBKT7, respectively. T-AD + 53-BD was used as a positive control. CC-EDR4, amino acids 1 to 149 of EDR4, which includes the CC domain; ΔCC-EDR4, a deletion variant of EDR4 protein, which lacks amino acids 1 to 149; LCR-EDR4, amino acids 150 to 491 of EDR4, which includes the four LCR domains; DUF-EDR4, amino acids 492 to 615 of EDR4, which includes the Duf3133 domain.
(B) EDR4 interacted with EDR1 in BiFC assays in *N. benthamiana*. EDR1 was fused to the N-terminal fragment of YFP, and EDR4 (full length or deletion form of EDR4) was fused to the C-terminal fragment of YFP. YFP fluorescence indicates an interaction between the two proteins. Bars = 50 μm.
(C) Expression and Co-IP of *pEDR1-EDR1-FLAG* and *pEDR4-EDR4-GFP* in Arabidopsis. Total protein was extracted from 4-week-old transgenic plants expressing both EDR1-FLAG and EDR4-GFP. Plants expressing EDR1-FLAG and GFP (left panels) were used as negative controls. The EDR1-FLAG protein was immunoprecipitated with anti-FLAG antibody, and the presence of EDR4-GFP or GFP protein was detected by immunoblot analysis with anti-GFP antibody. These experiments were repeated three times with similar results.

the 35S promoter and used the F2 plants that expressed both EDR4-GFP and MYC-N-CHC2 in Co-IP assays, with plants that expressed only MYC-N-CHC2 as a negative control. CHC2 was only detected in the precipitates of leaves that express EDR4-GFP and MYC-N-CHC2 but not in the negative control plants (Figure 8B), indicating that EDR4 interacts with CHC2 in Arabidopsis.

The *chc2* mutants display reduced endocytosis rates, as measured by uptake of the endocytic tracer dye FM4-64 (Kitakura et al., 2011). To assess whether EDR4 also functions in endocytosis, we

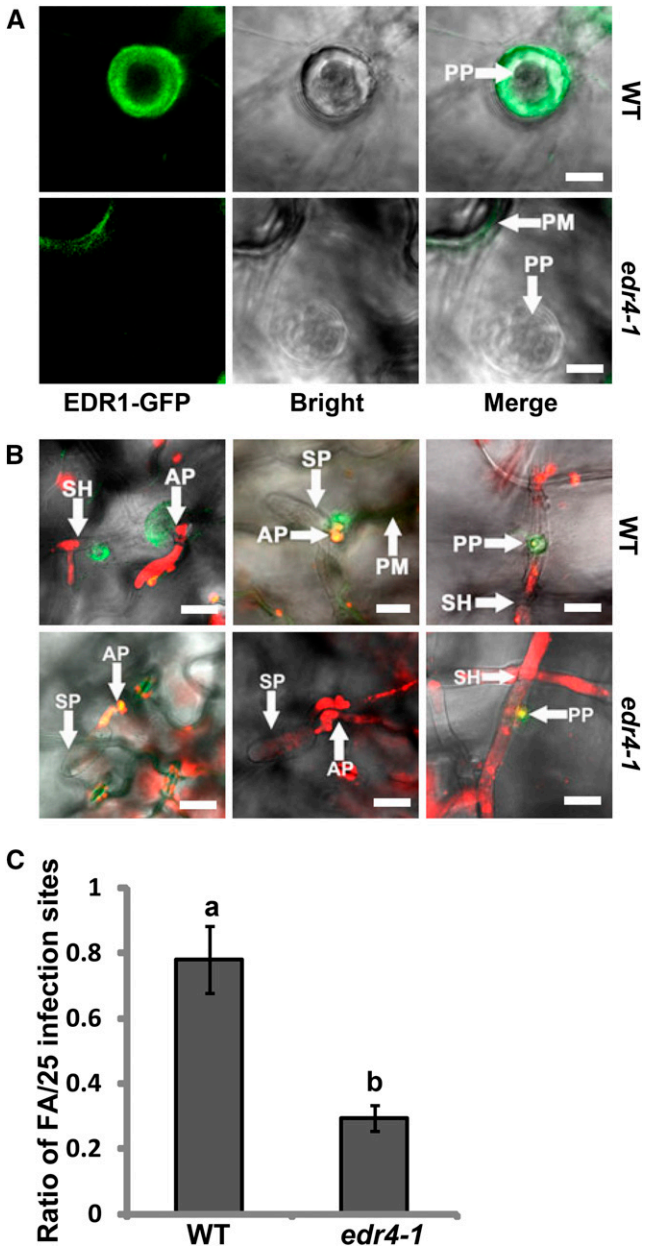

Figure 7. *edr4-1* Affects EDR1 Focal Accumulation at the Interface between the Powdery Mildew and Arabidopsis.

(A) and **(B)** Focal accumulation of EDR1-GFP at the pathogen infection site in epidermal cells of 4-week-old wild-type and *edr4-1* plants after inoculation with *G. cichoracearum*, shown in different views. Leaves were stained with propidium iodide in **(B)**. Fungal structures are shown in red. AP, appressoria; PM, plasma membrane; PP, penetration peg; SH, secondary hyphae; SP, spores. Bars = 20 μm.

(C) Quantitative analysis of powdery mildew-induced EDR1-GFP focal accumulations (FA) in wild-type and *edr4-1* mutant plants. The frequency was determined by counting the number of focal accumulations present in 25 random successful penetrations by appressoria per leaf, for three leaves per line. Bars represent means and SD of values obtained from three biological replicates per genotype. Statistically significant differences among the samples are labeled with different letters ($P < 0.01$, one-way ANOVA). The experiments were repeated three times with similar results.

performed FM4-64 uptake tests on wild-type, *edr4-1*, and *edr4-2* plants, using *chc2-1* as an endocytosis-deficient control. The intracellular accumulation of FM4-64 showed clear labeling of endosomes in the wild type within 8 min; however, *edr4-1*, *edr4-2*, and *chc2-1* mutants showed much less labeling at the same time (Figures 9A and 9B), indicating that *edr4* mutants show reduced endocytosis rates. By contrast, we did not observe any difference in FM4-64 uptake between the wild type and *edr1* mutants (Supplemental Figure 19). To examine whether CHC2 affects powdery mildew resistance, we infected the *chc2-1* and *chc2-2* mutants with *G. cichoracearum*. The *chc2-1* and *chc2-2* mutants supported significantly less fungal growth than the wild type, although the resistance in *chc2-1* and *chc2-2* mutants was not as strong as in the *edr4-1* mutant (Figures 9C and 9D). In addition, the *chc2-1* and *chc2-2* mutants showed higher H_2O_2 and callose accumulation and stronger activation of MPKs than the wild type (Supplemental Figure 20). The callose accumulation and activation of MPKs in *chc2-1* and *chc2-2* were similar to those in *edr4-1*, but the accumulation of H_2O_2 was significantly lower than that observed in *edr4-1* mutants (Supplemental Figure 20). Taken together, our data indicated that CHC2 contributes to powdery mildew resistance.

As the *chc2* mutants displayed an *edr4*-like phenotype, and CHC2 interacts with EDR4, we then asked whether CHC2 contributes to the relocation of EDR1 and EDR4 upon powdery mildew infection. To address this question, we transformed EDR1-GFP and EDR4-GFP constructs into *chc2-1*, to generate *chc2-1* EDR1-GFP and *chc2-1* EDR4-GFP transgenic plants. We then examined the localization of EDR1-GFP and EDR4-GFP in the *chc2-1* mutant. The localization of EDR1-GFP and EDR4-GFP was similar in wild-type and *chc2-1* plants before powdery mildew infection (Supplemental Figures 14B and 14C). However, both EDR1-GFP and EDR4-GFP accumulated at much lower levels at infection sites in *chc2-1* than wild-type leaves at 24 HAI (Figures 9E and 9G). Quantification analysis also confirmed those results (Figures 9F and 9H).

DISCUSSION

The loss-of-function mutants of *EDR4* showed enhanced resistance to *G. cichoracearum* and increased mildew-induced cell death. The *edr4*-mediated resistance included increased callose deposition, higher levels of H_2O_2, stronger activation of MPKs, enhanced expression of pathogenesis-related genes, and higher levels of SA, which are very similar to previously identified *edr1* mutants (Frye et al., 2001). Genetic analysis showed that *edr1*- and *edr4*-mediated resistance both require pathways induced by SA but not by JA or ethylene. In addition, the *edr1 edr4-1* double mutant displays a similar phenotype to *edr1* and *edr4-1* single mutants, and *keg-4* suppresses the double and single mutants (Wawrzynska et al., 2008). By contrast, although *edr2* also shares a similar phenotype with *edr1* and *edr4-1*, it appears that *edr4-1* and *edr2* function by different mechanisms, as the *edr2* mutation enhances *edr4*-mediated resistance and mildew-induced cell death phenotypes and *keg-4* suppresses *edr4-1* but not *edr2*. In

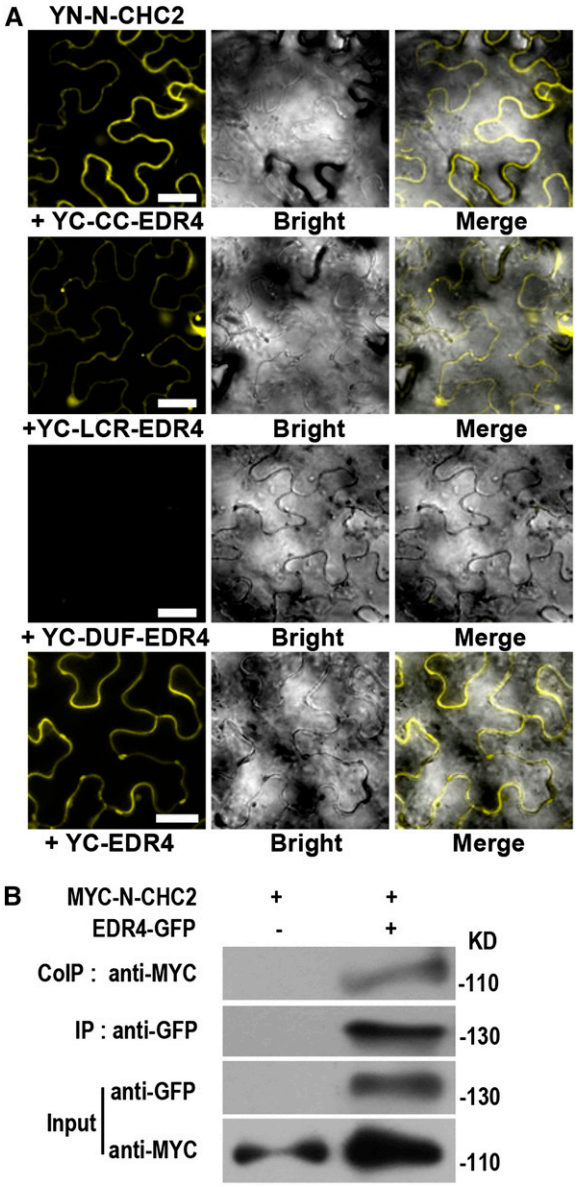

Figure 8. EDR4 Interacts with CHC2 in Vivo.

(A) BiFC assays in *N. benthamiana* show interactions between YN-N-CHC2 and YC-EDR4. The N-terminal domain (amino acids 1 to 1016) of CHC2 was fused to the N-terminal fragment of YFP, and the fragments, including full-length EDR4, the CC domain, four LCR domains, and the Duf3133 domain of EDR4, were fused to the C-terminal fragment of YFP. YFP fluorescence indicates an interaction between the two proteins. The experiments were repeated three times with similar results. Bars = 30 μm.

(B) Expression and Co-IP of *pEDR4-EDR4-GFP* and *35S-MYC-N-CHC2* in Arabidopsis. Total protein was extracted from 4-week-old transgenic plants expressing both EDR4-GFP and MYC-N-CHC2. The EDR4-GFP protein was immunoprecipitated with anti-GFP antibody, and the presence of MYC-N-CHC2 protein was detected by immunoblot analysis with anti-MYC antibody. The experiments were repeated three times with similar results.

addition, similar to the *edr1* mutant, *edr4*-mediated resistance also requires MPK3, MKK4, and MKK5. Taken together, these observations strongly suggest that *EDR1* and *EDR4* may function in the same pathway to regulate powdery mildew resistance and cell death, and this pathway requires KEG function.

EDR4 encodes an unknown protein, and its biological function is not clear; however, several lines of evidence suggest that EDR4 may contribute to clathrin-mediated pathways. First, EDR4 interacts with CHC2, the clathrin-coated vesicle component in clathrin-mediated pathways (Arabidopsis Interactome Mapping Consortium, 2011). Second, EDR4-GFP shows intracellular movement. Third, *edr4* mutants display defects in FM4-64 uptake, similar to the phenotype of *chc2* mutants (Kitakura et al., 2011). In plants, several evolutionarily conserved CME components have already been identified, including clathrin, the actin cytoskeleton, dynamin-related proteins, and accessory adaptor proteins (Chen et al., 2011). One possibility is that EDR4 may function as an accessory adaptor protein, which links cargo to clathrin and transports the associated cargo to its destination, although more evidence is needed to support this hypothesis.

Increasing evidence shows that vesicle trafficking plays important roles in plant defense. For example, PEN1-mediated vesicle trafficking is important for nonhost resistance (Nielsen and Thordal-Christensen, 2013), and MIN7-mediated vesicle trafficking contributes to resistance to bacterial pathogens (Nomura et al., 2011). In addition, internalization of FLS2 by vesicle trafficking is also critical for the activation of FLS2-mediated responses (Robatzek et al., 2006). However, PEN1- and MIN7-mediated vesicle trafficking, as well as internalization of FLS2, all play positive roles in plant immunity. By contrast, loss-of-function mutation of *EDR4* leads to enhanced disease resistance, suggesting that EDR4 plays a negative role in plant immunity. Similarly, mutations in CHC2, the heavy chain of clathrin, which associates with EDR4, also show enhanced disease resistance to powdery mildew, suggesting a negative role of CHC2 in powdery mildew resistance. Why does EDR4-mediated vesicle trafficking have negative effects on plant immunity? The simplest explanation is that resistance in *edr4* results from the mislocalization of EDR1, a negative regulator of defense responses, as EDR4 may help to transport EDR1 to the infection site. Recently, we showed that EDR1 interacts with MKK4/MKK5 and negatively affects the MAPK cascade to fine-tune plant disease resistance (Zhao et al., 2014). In this context, EDR1 transport to the fungal infection site likely keeps the activation of the MAPK pathway at low levels. By contrast, in *edr4* mutants, failure to transport EDR1 to the infection site results in MAPK pathway activation to high levels, which leads to the enhanced resistance and cell death in *edr4* mutants, similar to *edr1*. However, it is worthwhile to note that the *chc2* mutant did not show strong resistance to powdery mildew, in contrast with the *edr4* mutant, indicating that factors in addition to the reduced recruitment of EDR1 to the sites of penetration cause the enhanced disease resistance phenotype of the *edr4* mutants.

Similar to EDR1 and EDR4, PEN1 accumulates at penetration sites upon powdery mildew infection. However, PEN1 accumulates at both papillae and plasma membrane at *B. graminis* f sp *hordei* penetration sites (Meyer et al., 2009), while EDR1 and EDR4 accumulate on the plasma membrane but not at papillae. Recent work shows that the accumulation of PEN1 on papillae may have no direct effect on penetration resistance; instead, PEN1 may

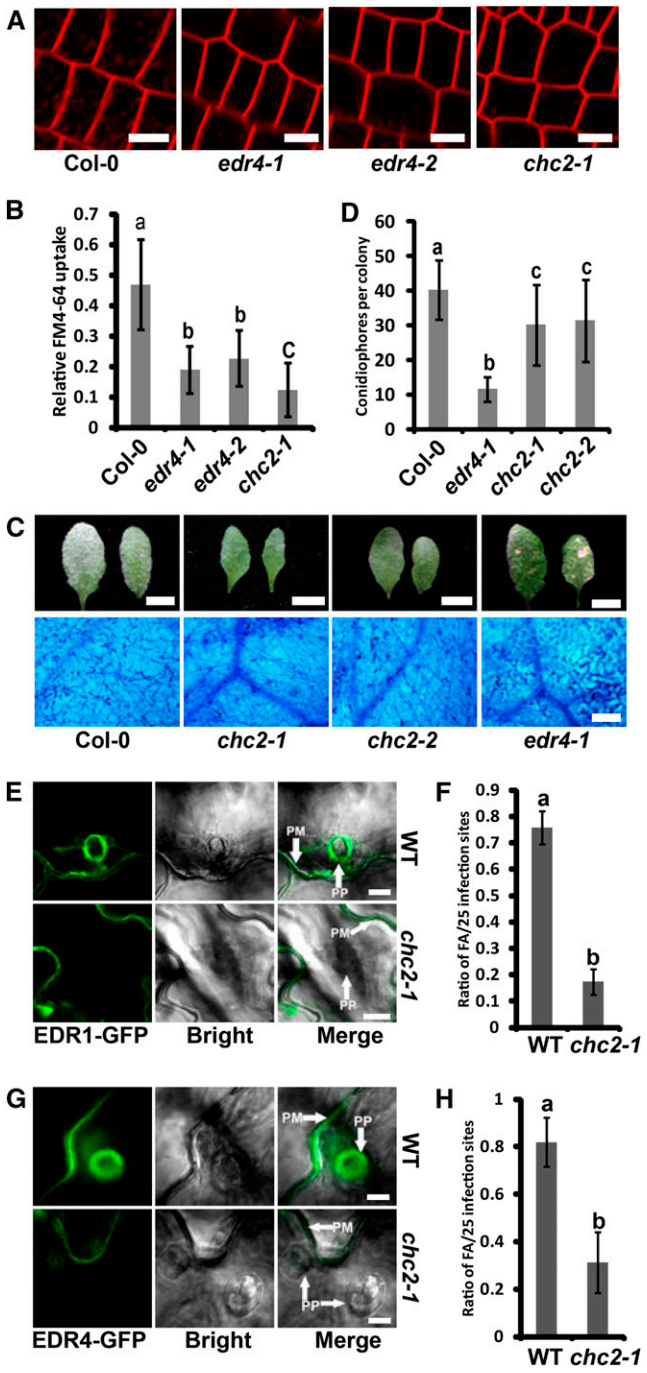

Figure 9. *edr4* Mutants Show Defects in FM4-64 Uptake; Focal Accumulation of EDR1 and EDR4 Requires CHC2.

(A) Delay of FM4-64 uptake in the *edr4* mutants. Intracellular accumulation of FM4-64 was examined at 8 min after staining with 2 μM FM4-64 in root tip cells of 5-d-old seedlings of the wild type and *edr4-1*, *edr4-2*, and *chc2-1* mutants. Bars = 10 μm.

(B) Quantification of relative FM4-64 uptake. The bars represent means and SD (n > 50 cells analyzed). Statistically significant differences among the samples are labeled with different letters ($P < 0.01$, one-way ANOVA). The experiments were repeated three times with similar results.

function on the endosome and *trans*-Golgi network, and recycling mediated by PEN1 could be an important response to fungal infection (Nielsen and Thordal-Christensen, 2013). In this context, recycling of EDR1 by an EDR4-mediated pathway could play an important role in the negative regulation of powdery mildew resistance. Regarding recycling of EDR1, one important question is why plants need to transport a negative regulator of defense to infection sites to suppress immunity. One possible explanation is that plants have developed sophisticated mechanisms to regulate innate immunity, in which many positive and negative regulators are recruited and deployed at the infection sites, thus allowing the plant to fine-tune its defenses in response to different situations. Deployment of the negative regulators to the infection site could prevent inappropriate activation of plant immunity or limit plant immunity to appropriate levels.

KEG plays a critical role in multiple intracellular trafficking processes, including vacuole biogenesis, targeting of membrane-associated proteins to the vacuole, and secretion of apoplastic proteins (Gu and Innes, 2012). Mutation of *KEG* specifically suppresses *edr1*-mediated resistance, but how KEG affects *edr1*-mediated defenses remains unclear. KEG associates with EDR1 and also moves to the site of infection (Gu and Innes, 2012). Although KEG does not physically associate with EDR4, it will be interesting to see whether the movement of KEG to the *G. cichoracearum* infection sites requires EDR4. Recently, ATL1 was identified as a potential substrate of EDR1. ATL1 interacts with EDR1 in the TGN/EE and constitutively cycles between the plasma membrane and the TGN/EE (Serrano et al., 2014). It would be interesting to examine whether *edr4*-mediated powdery mildew resistance requires ATL1 and whether EDR4 contributes to the recycling of ATL1.

The resistance and cell death mediated by *edr1* and *edr4* require intact SA signaling. SA interferes with endocytosis and affects the cycling of proteins at the plasma membrane (Du et al., 2013). Also, the impact of SA on endocytosis involves clathrin, as clathrin mutants show less sensitivity to SA. Interestingly, the effect of SA on CME does not require NPR1, indicating that SA affects CME by different mechanisms and is not involved in transcriptional regulation by NPR1. This suggests that CME has a complicated role in

(C) Photographs and trypan blue staining of representative leaves removed from 4-week-old wild-type, *chc2-1*, *chc2-2*, and *edr4-1* plants at 8 DAI with *G. cichoracearum*. Bars in top panels = 0.5 cm; bar in bottom panels = 100 μm.

(D) Quantitative analysis of conidiophore formation on 4-week-old wild-type, *chc2-1*, *chc2-2*, and *edr4-1* plants inoculated with *G. cichoracearum* at 6 DAI. The bars represent means and SD. The experiment was repeated three times with similar results (n = 20). Statistically significant differences are labeled with different letters ($P < 0.01$, one-way ANOVA). The experiments were repeated three times with similar results.

(E) and **(G)** Focal accumulation of EDR1-GFP **(E)** or EDR4-GFP **(G)** at the pathogen infection site in epidermal cells of 4-week-old wild-type and *chc2-1* plants after inoculation with *G. cichoracearum* at 24 HAI. PM, plasma membrane; PP, penetration peg. Bars = 10 μm.

(F) and **(H)** Quantitative analysis of powdery mildew-induced EDR1-GFP **(F)** or EDR4-GFP **(H)** focal accumulations (FA) in wild-type and *chc2-1* plants. Bars represent means and SD of values obtained from three biological replicates per genotype. Statistically significant differences among the samples are labeled with different letters ($P < 0.01$, one-way ANOVA). The experiments were repeated three times with similar results.

plant immunity; for example, it remains to be tested whether SA affects an EDR4-mediated pathway and whether the interference of CME by SA represents a novel mechanism for SA regulation of plant immunity.

In this study, we demonstrated that EDR4 plays important roles in plant disease resistance and regulates EDR1 focal accumulation by forming a complex to affect plant defenses. However, several questions remain to be answered. Does EDR4 play a role in clathrin-mediated pathways? What are the other proteins that EDR4 helps to relocate? Does EDR4 contribute to CME? Answering these questions will increase our understanding of the functions of clathrin-mediated pathways in plant immunity.

METHODS

Plant Growth and Materials

Arabidopsis thaliana seeds were surface-sterilized and chilled at 4°C for 3 d, then sown on plates containing half-strength Murashige and Skoog medium with 1% sucrose. For phenotyping, plants were grown in a growth room with a 9-h-light/15-h-dark photoperiod, light intensity of 7000 to 8000 lux, and relative humidity of 50 to 60% at 21 to 24°C. Seedlings were transplanted into soil 7 d after germination. For seed set, the plants were placed in a growth room at 21 to 24°C with a long-day photoperiod (16-h-light/8-h-dark cycle). *Nicotiana benthamiana* plants used for transient expression were grown under the same short-day conditions as Arabidopsis.

Powdery Mildew Infections

Four-week-old plants were inoculated with *Golovinomyces cichoracearum*, and the number of conidiophores per colony was counted at 6 DAI, as described previously (Wang et al., 2011). Trypan blue staining was used to monitor the fungal structures and dead plant cells (Frye and Innes, 1998). H_2O_2 accumulation was detected by staining with DAB (Xiao et al., 2005), and callose deposition was detected by aniline blue staining (Pan et al., 2012). Quantitative analysis of callose and H_2O_2 accumulation followed the method described previously (Zhang et al., 2007; Yoshimoto et al., 2009). The samples were observed and photographed with an Olympus BX53 microscope.

Construction of Double Mutants

Double and triple mutants were created by standard genetic crosses with previously described mutant alleles, including *eds1-2* (Bartsch et al., 2006), *eds5-1* (Nawrath et al., 2002), *pad4-1* (Jirage et al., 1999), *npr1-63* (Alonso et al., 2003), *coi1-1* (Xie et al., 1998), *ein2-1* (Guzmán and Ecker, 1990), *sid2-2* (Wildermuth et al., 2001), *edr1* (Frye et al., 2001), *edr1-2* (Hiruma et al., 2011), *edr2* (Tang et al., 2005), *keg-4* (Wawrzynska et al., 2008), *chc2-1* and *chc2-2* (Kitakura et al., 2011), *mpk3-1* and *mpk6-3* (Bartels et al., 2009), and *mkk4-18* and *mkk5-18* (Zhao et al., 2014). All the plants used were in the Col-0 background, except for *coi1-1* (in the Columbia-6 background). The genotypes of mutants were confirmed by PCR using the primers listed in Supplemental Table 1.

Map-Based Cloning of *EDR4*

To map *EDR4*, *edr4-1* was crossed with Landsberg *erecta* to generate a segregating population. Initially, the *edr4-1* mutation was mapped between markers CTR1 and CIW14 on chromosome 5. Fine-mapping narrowed the mutation to a 50-kb interval spanning the 3′ end of BAC clone K2A11 (GenBank accession number AB018111.1) and the 5′ end of BAC K18I23 (GenBank accession number AB010692.1). We subsequently amplified and sequenced all 19 predicted genes in this region.

For complementation analysis, a 5.0-kb genomic DNA of At5g05190 from the wild type was amplified and inserted into the pCAMBIA1300 vector. The constructs were verified by sequencing and introduced into *Agrobacterium tumefaciens* GV3101, then transformed into *edr4-1* plants using the floral dip method (Clough and Bent, 1998). Transgenic plants were selected on half-strength Murashige and Skoog medium containing 50 mg/L hygromycin (Sigma-Aldrich). Transformants were transplanted to soil 7 d after germination, and T1 transgenic plants were used for phenotyping.

The primers used are listed in Supplemental Table 1.

Real-Time PCR Analysis and SA Quantification

Real-time PCR to measure transcript accumulation was performed as described (Nie et al., 2012). SA extraction and measurement were performed as described (Gou et al., 2009).

Confocal Microscopy and FRAP

To produce the *pEDR4-EDR4-GFP* construct, the genomic sequence or coding sequence (CDS) without the stop codon of *EDR4* was amplified (primer sequences are listed in Supplemental Table 1) and cloned into the Gateway entry vector pDONR207 using the BP Clonase kit (Invitrogen). The fragment was then cloned into pMDC107 with the LR Clonase kit (Invitrogen). The constructs were introduced into Agrobacterium strain GV3101 and then transformed into the *edr4-1* mutant. Similarly, Δ*CC-EDR4* (CC domain deletion) was cloned into pEarleyGate302 vector with *EDR4* promoter and C-terminal FLAG fusion. The *pEDR1-EDR1-GFP* (Zhao et al., 2014) and *NAG-GFP* (Essl et al., 1999) lines were described previously. The TGN/EE and late endosome markers SYP61 and ARA6 (Gu and Innes, 2011, 2012; Serrano et al., 2014) were introduced into EDR4-GFP plants by transformation, respectively. The ER marker line expressing HDEL-mCherry and the *cis*-Golgi marker line expressing SYP32-mCherry (Nelson et al., 2007; Geldner et al., 2009) were introduced into EDR4-GFP plants by genetic crosses. Confocal imaging was performed on an inverted Zeiss LSM 710 NLO microscope with ZEN 2009 software. Quantification of colocalization was performed as described previously (Herda et al., 2012). To visualize fungal structures, the infected leaves were stained with 0.01 mg/mL propidium iodide for 15 min (Ramonell et al., 2005). Calculating the focal accumulations of EDR1-GFP upon powdery mildew infection was performed as described previously (Underwood and Somerville, 2013).

FRAP assays were performed on a region of focal accumulation or a distal plasma membrane site as described previously (Bhat et al., 2005). Briefly, Arabidopsis leaves were bleached using the 488-nm argon laser line 50 times at 100% intensity. Images were collected 2 min before bleaching and at different time points after bleaching. Fluorescence intensity at each time point for each bleached site was determined using ImageJ software. Relative intensity values were normalized based on focal accumulation before and after bleaching.

FM4-64 Uptake Assay

The FM4-64 uptake assay was performed as described previously, with minor changes (Kitakura et al., 2011). Five-day-old seedlings were incubated with 2 μM FM4-64 for 8 min. The roots of seedlings were observed by confocal microscopy. The mean pixel intensity of the cytosolic side of cells and the adjacent plasma membrane was measured with ImageJ. Then, the quotients of values for the cytosolic side and the plasma membrane were calculated.

Plasmolysis

The plasmolysis assay was performed as described previously (Underwood and Somerville, 2013). For plasmolysis observation, Arabidopsis leaves infected with *G. cichoracearum* at 24 HAI were soaked in 0.85 M NaCl for 15 min and then observed by confocal microscopy.

MAPK Assay

Total protein from leaves was extracted as described (Liu et al., 2010). The activated MAPKs were detected using anti-pTEpY primary antibodies (Cell Signaling Technology).

Yeast Two-Hybrid Assays

CDSs of *EDR1*, *EDR1* N-terminal domain, and *EDR1* C-terminal domain were cloned into pGBKT7 (Zhao et al., 2014). CDSs of *KEG*, *EDR4*, and deletion variants of *EDR4* were amplified and ligated into pGADT7. The CDS of *EDR4* was also cloned into pGBKT7. The plasmids were cotransformed into yeast strain Y190, and positive clones were selected on SD/-Leu/-Trp medium and then verified by PCR amplification of both cotransformed genes. Verified clones were selected on SD/-Leu/-Trp/-His medium with 25 mM 3-amino-1,2,4-triazole (Sigma-Aldrich) and stained with 40 μg/mL X-Gal (Clontech) to determine β-galactosidase activity.

BiFC Analysis

35S-YN-EDR1 was described previously (Zhao et al., 2014). To generate *35S*-YC fusion constructs, CDSs of *KEG*, *EDR4*, and the deletion variants of *EDR4* were cloned into pSY735 (Bracha-Drori et al., 2004) in frame with YFP^C. Then, the fusion sequences were amplified and cloned into the binary vector pMDC32. Similarly, to generate *35S-YN-N-CHC2* and *35S-YN-KEG*, CDSs of *CHC2* (encoding the N-terminal domain amino acids 1 to 1016 of CHC2) and *KEG* were first cloned into pSY736 in frame with YFP^N and then cloned into pMDC32. The plasmid was subsequently introduced into Agrobacterium strain GV3101. Reconstitution of YFP fluorescence was examined by transient coexpression in 4-week-old *N. benthamiana* by infiltration with Agrobacterium strain GV3101 carrying different YFP^N and YFP^C pairs, as described (Zhao et al., 2014). Samples were observed by confocal microscopy 2 DAI.

Protein Extraction and Co-IP Assays

For EDR1 and EDR4 Co-IP assays in Arabidopsis, transgenic *edr1* plants expressing *pEDR1-EDR1-FLAG* (Zhao et al., 2014) were crossed with *edr4-1* plants expressing *pEDR4-EDR4-GFP* or *35S-GFP*. The leaf samples were from 4-week-old F2 plants expressing both EDR1-FLAG and EDR4-GFP or F1 plants expressing EDR1-FLAG and GFP. For CHC2 and EDR4 Co-IP assays in Arabidopsis, CDS of *CHC2* (encoding the N-terminal domain amino acids 1 to 1016 of CHC2) was cloned into pEarleyGate203 vector with the 35S promoter and N-terminal MYC tag. The derived *35S-MYC-N-CHC2* construct was transformed into Col-0 plants, and the transgenic plants were then crossed with EDR4-GFP plants. The leaves from 4-week-old F2 plants expressing both MYC-N-CHC2 and EDR4-GFP or MYC-N-CHC2 were used for Co-IP assays. The protein was extracted using NB1 buffer plus 0.2% (v/v) IGEPAL CA-630 (Sigma-Aldrich) (Liu et al., 2010), and Co-IP assays were performed as described previously (Shi et al., 2013).

Accession Numbers

Sequence data from this article can be found in the Arabidopsis Genome Initiative or GenBank/EMBL databases under the following accession numbers: EDR4 (AT5G05190), SYP32 (AT3G24350), SYP61 (AT1G28490), ARA6 (AT3G54840), PEN1 (AT3G11820), EDR1 (AT1G08720), KEG (AT5G13530), CHC2 (AT3G08530), ACT2 (AT3G18780), PR1 (AT2G14610), PR2 (AT3G57260), and PR5 (AT1G75040).

Supplemental Data

Supplemental Figure 1. The Growth Phenotype of *edr4-1* Mutants under Short and Long Day Conditions.

Supplemental Figure 2. Quantification of H_2O_2 and Callose Accumulation in *edr4-1* after *G. cichoracearum* Infection.

Supplemental Figure 3. Quantitative Analysis of Conidiophore Formation on Inoculated Leaves of Wild Type, *edr4-1*, and Different Double Mutant Plants with *G. cichoracearum* at 6 DAI.

Supplemental Figure 4. Identification and Complementation of the *edr4-1* Mutation.

Supplemental Figure 5. EDR4-GFP Fusion Protein Complemented the *edr4-1* Powdery Mildew Resistance Phenotype.

Supplemental Figure 6. Selected Frames of Supplemental Movies 1, 2, and 3.

Supplemental Figure 7. NAG-GFP Proteins Did Not Accumulate at the Penetration Site upon *G. cichoracearum* Infection.

Supplemental Figure 8. EDR4 and EDR1 Localize to the Plasma Membrane, Not Papillae.

Supplemental Figure 9. The *edr2* Mutation Enhances the *edr4*-Mediated Powdery Mildew Resistance Phenotype.

Supplemental Figure 10. *edr4*-Mediated Resistance Requires the MAPK Pathway.

Supplemental Figure 11. EDR4 Interacts with N-Terminal Domain of EDR1 in Yeast Two-Hybrid Assays.

Supplemental Figure 12. EDR4 Interacts with EDR1, Not KEG, in Vivo.

Supplemental Figure 13. EDR4 Colocalizes with EDR1.

Supplemental Figure 14. The *edr4-1* and *chc2-1* Mutations Did Not Affect EDR1-GFP Localization in Uninfected Leaves.

Supplemental Figure 15. The EDR4 Coiled-Coil Domain Is Required for EDR4 Function.

Supplemental Figure 16. EDR1-GFP Localization in an EDR4-CC-Domain Deletion Background.

Supplemental Figure 17. The *edr1-1* Mutation Did Not Affect EDR4-GFP Localization in Uninfected and Infected Leaves.

Supplemental Figure 18. FRAP Analysis of EDR1-GFP and EDR4-GFP Focal Accumulation at Powdery Mildew Penetration Sites.

Supplemental Figure 19. The *edr1* Mutant Did Not Show Defects in FM4-64 Uptake.

Supplemental Figure 20. The *chc2* Mutants Show Increased Accumulation of H_2O_2 and Callose Deposition and Stronger MPK Activation.

Supplemental Table 1. Primers Used in This Study.

Supplemental Movie 1. EDR4-GFP Intracellular Trafficking in a Root Cell.

Supplemental Movie 2. EDR4-GFP Intracellular Trafficking in an Epidermal Cell.

Supplemental Movie 3. EDR1-GFP Intracellular Trafficking in an Epidermal Cell.

ACKNOWLEDGMENTS

We thank Roger Innes for *edr4-1* seeds and mCherry-SYP61 and ARA6-mCherry plasmids, Jiri Friml for *chc2-1* and *chc2-2* seeds, Jinlong Qiu for PEN1-GFP seeds, Lei Ge for HDEL-mCherry and NAG-GFP seeds, and the ABRC and Nottingham Arabidopsis Stock Centre for SYP32-mCherry and T-DNA insertion lines. We thank Hui Liang for assistance

with confocal microscopy. This work was supported by the Strategic Priority Research Program of the Chinese Academy of Sciences (Grant XDB11020100), the National Basic Research Program of China (Grant 2015CB910200), and the National Natural Science Foundation of China (Grant 31171160).

AUTHOR CONTRIBUTIONS

D.T. and G.W. initiated the project and designed the experiments. G.W., S.L., Y.Z., and W.W. performed the research. D.T., G.W., and Z.K. analyzed data. D.T. and G.W. wrote the article.

Received December 8, 2014; revised February 17, 2015; accepted February 22, 2015; published March 6, 2015.

REFERENCES

Alonso, J.M., et al. (2003). Genome-wide insertional mutagenesis of *Arabidopsis thaliana*. Science **301:** 653–657.

Arabidopsis Interactome Mapping Consortium (2011). Evidence for network evolution in an Arabidopsis interactome map. Science **333:** 601–607.

Bartels, S., Anderson, J.C., González Besteiro, M.A., Carreri, A., Hirt, H., Buchala, A., Métraux, J.P., Peck, S.C., and Ulm, R. (2009). MAP kinase phosphatase1 and protein tyrosine phosphatase1 are repressors of salicylic acid synthesis and SNC1-mediated responses in *Arabidopsis*. Plant Cell **21:** 2884–2897.

Bartsch, M., Gobbato, E., Bednarek, P., Debey, S., Schultze, J.L., Bautor, J., and Parker, J.E. (2006). Salicylic acid-independent ENHANCED DISEASE SUSCEPTIBILITY1 signaling in *Arabidopsis* immunity and cell death is regulated by the monooxygenase FMO1 and the Nudix hydrolase NUDT7. Plant Cell **18:** 1038–1051.

Bhat, R.A., Miklis, M., Schmelzer, E., Schulze-Lefert, P., and Panstruga, R. (2005). Recruitment and interaction dynamics of plant penetration resistance components in a plasma membrane microdomain. Proc. Natl. Acad. Sci. USA **102:** 3135–3140.

Boller, T., and Felix, G. (2009). A renaissance of elicitors: Perception of microbe-associated molecular patterns and danger signals by pattern-recognition receptors. Annu. Rev. Plant Biol. **60:** 379–406.

Bracha-Drori, K., Shichrur, K., Katz, A., Oliva, M., Angelovici, R., Yalovsky, S., and Ohad, N. (2004). Detection of protein-protein interactions in plants using bimolecular fluorescence complementation. Plant J. **40:** 419–427.

Burkhard, P., Stetefeld, J., and Strelkov, S.V. (2001). Coiled coils: A highly versatile protein folding motif. Trends Cell Biol. **11:** 82–88.

Chen, X., Irani, N.G., and Friml, J. (2011). Clathrin-mediated endocytosis: The gateway into plant cells. Curr. Opin. Plant Biol. **14:** 674–682.

Chinchilla, D., Zipfel, C., Robatzek, S., Kemmerling, B., Nürnberger, T., Jones, J.D.G., Felix, G., and Boller, T. (2007). A flagellin-induced complex of the receptor FLS2 and BAK1 initiates plant defence. Nature **448:** 497–500.

Clough, S.J., and Bent, A.F. (1998). Floral dip: A simplified method for Agrobacterium-mediated transformation of *Arabidopsis thaliana*. Plant J. **16:** 735–743.

Collins, N.C., Thordal-Christensen, H., Lipka, V., Bau, S., Kombrink, E., Qiu, J.L., Hückelhoven, R., Stein, M., Freialdenhoven, A., Somerville, S.C., and Schulze-Lefert, P. (2003). SNARE-protein-mediated disease resistance at the plant cell wall. Nature **425:** 973–977.

Dhonukshe, P., Aniento, F., Hwang, I., Robinson, D.G., Mravec, J., Stierhof, Y.D., and Friml, J. (2007). Clathrin-mediated constitutive endocytosis of PIN auxin efflux carriers in Arabidopsis. Curr. Biol. **17:** 520–527.

Du, Y., Tejos, R., Beck, M., Himschoot, E., Li, H., Robatzek, S., Vanneste, S., and Friml, J. (2013). Salicylic acid interferes with clathrin-mediated endocytic protein trafficking. Proc. Natl. Acad. Sci. USA **110:** 7946–7951.

Essl, D., Dirnberger, D., Gomord, V., Strasser, R., Faye, L., Glössl, J., and Steinkellner, H. (1999). The N-terminal 77 amino acids from tobacco N-acetylglucosaminyltransferase I are sufficient to retain a reporter protein in the Golgi apparatus of *Nicotiana benthamiana* cells. FEBS Lett. **453:** 169–173.

Frye, C.A., and Innes, R.W. (1998). An *Arabidopsis* mutant with enhanced resistance to powdery mildew. Plant Cell **10:** 947–956.

Frye, C.A., Tang, D., and Innes, R.W. (2001). Negative regulation of defense responses in plants by a conserved MAPKK kinase. Proc. Natl. Acad. Sci. USA **98:** 373–378.

Gadeyne, A., et al. (2014). The TPLATE adaptor complex drives clathrin-mediated endocytosis in plants. Cell **156:** 691–704.

Geldner, N., Dénervaud-Tendon, V., Hyman, D.L., Mayer, U., Stierhof, Y.D., and Chory, J. (2009). Rapid, combinatorial analysis of membrane compartments in intact plants with a multicolor marker set. Plant J. **59:** 169–178.

Gou, M., Su, N., Zheng, J., Huai, J., Wu, G., Zhao, J., He, J., Tang, D., Yang, S., and Wang, G. (2009). An F-box gene, CPR30, functions as a negative regulator of the defense response in Arabidopsis. Plant J. **60:** 757–770.

Gu, Y., and Innes, R.W. (2011). The KEEP ON GOING protein of Arabidopsis recruits the ENHANCED DISEASE RESISTANCE1 protein to trans-Golgi network/early endosome vesicles. Plant Physiol. **155:** 1827–1838.

Gu, Y., and Innes, R.W. (2012). The KEEP ON GOING protein of *Arabidopsis* regulates intracellular protein trafficking and is degraded during fungal infection. Plant Cell **24:** 4717–4730.

Guzmán, P., and Ecker, J.R. (1990). Exploiting the triple response of *Arabidopsis* to identify ethylene-related mutants. Plant Cell **2:** 513–523.

Herda, S., Raczkowski, F., Mittrücker, H.W., Willimsky, G., Gerlach, K., Kühl, A.A., Breiderhoff, T., Willnow, T.E., Dörken, B., Höpken, U.E., and Rehm, A. (2012). The sorting receptor Sortilin exhibits a dual function in exocytic trafficking of interferon-γ and granzyme A in T cells. Immunity **37:** 854–866.

Hiruma, K., Nishiuchi, T., Kato, T., Bednarek, P., Okuno, T., Schulze-Lefert, P., and Takano, Y. (2011). Arabidopsis ENHANCED DISEASE RESISTANCE 1 is required for pathogen-induced expression of plant defensins in nonhost resistance, and acts through interference of MYC2-mediated repressor function. Plant J. **67:** 980–992.

Hong, Z., Bednarek, S.Y., Blumwald, E., Hwang, I., Jurgens, G., Menzel, D., Osteryoung, K.W., Raikhel, N.V., Shinozaki, K., Tsutsumi, N., and Verma, D.P. (2003). A unified nomenclature for Arabidopsis dynamin-related large GTPases based on homology and possible functions. Plant Mol. Biol. **53:** 261–265.

Hückelhoven, R., and Panstruga, R. (2011). Cell biology of the plant-powdery mildew interaction. Curr. Opin. Plant Biol. **14:** 738–746.

Jirage, D., Tootle, T.L., Reuber, T.L., Frost, L.N., Feys, B.J., Parker, J.E., Ausubel, F.M., and Glazebrook, J. (1999). *Arabidopsis thaliana* PAD4 encodes a lipase-like gene that is important for salicylic acid signaling. Proc. Natl. Acad. Sci. USA **96:** 13583–13588.

Jones, J.D.G., and Dangl, J.L. (2006). The plant immune system. Nature **444:** 323–329.

Kitakura, S., Vanneste, S., Robert, S., Löfke, C., Teichmann, T., Tanaka, H., and Friml, J. (2011). Clathrin mediates endocytosis and polar distribution of PIN auxin transporters in *Arabidopsis*. Plant Cell **23:** 1920–1931.

Koh, S., André, A., Edwards, H., Ehrhardt, D., and Somerville, S. (2005). *Arabidopsis thaliana* subcellular responses to compatible *Erysiphe cichoracearum* infections. Plant J. **44:** 516–529.

Lee, H.Y., Bowen, C.H., Popescu, G.V., Kang, H.G., Kato, N., Ma, S., Dinesh-Kumar, S., Snyder, M., and Popescu, S.C. (2011). *Arabidopsis* RTNLB1 and RTNLB2 Reticulon-like proteins regulate intracellular trafficking and activity of the FLS2 immune receptor. Plant Cell **23:** 3374–3391.

Lipka, V., et al. (2005). Pre- and postinvasion defenses both contribute to nonhost resistance in Arabidopsis. Science **310:** 1180–1183.

Liu, L., Zhang, Y., Tang, S., Zhao, Q., Zhang, Z., Zhang, H., Dong, L., Guo, H., and Xie, Q. (2010). An efficient system to detect protein ubiquitination by agroinfiltration in *Nicotiana benthamiana*. Plant J. **61:** 893–903.

Lu, D., Wu, S., Gao, X., Zhang, Y., Shan, L., and He, P. (2010). A receptor-like cytoplasmic kinase, BIK1, associates with a flagellin receptor complex to initiate plant innate immunity. Proc. Natl. Acad. Sci. USA **107:** 496–501.

McMahon, H.T., and Boucrot, E. (2011). Molecular mechanism and physiological functions of clathrin-mediated endocytosis. Nat. Rev. Mol. Cell Biol. **12:** 517–533.

Meyer, D., Pajonk, S., Micali, C., O'Connell, R., and Schulze-Lefert, P. (2009). Extracellular transport and integration of plant secretory proteins into pathogen-induced cell wall compartments. Plant J. **57:** 986–999.

Nawrath, C., Heck, S., Parinthawong, N., and Métraux, J.P. (2002). EDS5, an essential component of salicylic acid-dependent signaling for disease resistance in *Arabidopsis*, is a member of the MATE transporter family. Plant Cell **14:** 275–286.

Nelson, B.K., Cai, X., and Nebenführ, A. (2007). A multicolored set of in vivo organelle markers for co-localization studies in Arabidopsis and other plants. Plant J. **51:** 1126–1136.

Nie, H., Zhao, C., Wu, G., Wu, Y., Chen, Y., and Tang, D. (2012). SR1, a calmodulin-binding transcription factor, modulates plant defense and ethylene-induced senescence by directly regulating NDR1 and EIN3. Plant Physiol. **158:** 1847–1859.

Nielsen, M.E., and Thordal-Christensen, H. (2013). Transcytosis shuts the door for an unwanted guest. Trends Plant Sci. **18:** 611–616.

Nomura, K., Debroy, S., Lee, Y.H., Pumplin, N., Jones, J., and He, S.Y. (2006). A bacterial virulence protein suppresses host innate immunity to cause plant disease. Science **313:** 220–223.

Nomura, K., Mecey, C., Lee, Y.N., Imboden, L.A., Chang, J.H., and He, S.Y. (2011). Effector-triggered immunity blocks pathogen degradation of an immunity-associated vesicle traffic regulator in Arabidopsis. Proc. Natl. Acad. Sci. USA **108:** 10774–10779.

Pan, H., Liu, S., and Tang, D. (2012). HPR1, a component of the THO/TREX complex, plays an important role in disease resistance and senescence in Arabidopsis. Plant J. **69:** 831–843.

Panstruga, R., and Dodds, P.N. (2009). Terrific protein traffic: The mystery of effector protein delivery by filamentous plant pathogens. Science **324:** 748–750.

Puntervoll, P., et al. (2003). ELM server: A new resource for investigating short functional sites in modular eukaryotic proteins. Nucleic Acids Res. **31:** 3625–3630.

Ramonell, K., Berrocal-Lobo, M., Koh, S., Wan, J., Edwards, H., Stacey, G., and Somerville, S. (2005). Loss-of-function mutations in chitin responsive genes show increased susceptibility to the powdery mildew pathogen *Erysiphe cichoracearum*. Plant Physiol. **138:** 1027–1036.

Robatzek, S. (2014). Endocytosis: At the crossroads of pattern recognition immune receptors and pathogen effectors. In Applied Plant Cell Biology, P. Nick and Z. Opatrny, eds (Berlin: Springer), pp. 273–297.

Robatzek, S., Chinchilla, D., and Boller, T. (2006). Ligand-induced endocytosis of the pattern recognition receptor FLS2 in Arabidopsis. Genes Dev. **20:** 537–542.

Sauer, M., Delgadillo, M.O., Zouhar, J., Reynolds, G.D., Pennington, J.G., Jiang, L., Liljegren, S.J., Stierhof, Y.D., De Jaeger, G., Otegui, M.S., Bednarek, S.Y., and Rojo, E. (2013). MTV1 and MTV4 encode plant-specific ENTH and ARF GAP proteins that mediate clathrin-dependent trafficking of vacuolar cargo from the *trans*-Golgi network. Plant Cell **25:** 2217–2235.

Schulze-Lefert, P., and Panstruga, R. (2011). A molecular evolutionary concept connecting nonhost resistance, pathogen host range, and pathogen speciation. Trends Plant Sci. **16:** 117–125.

Serrano, I., Gu, Y., Qi, D., Dubiella, U., and Innes, R.W. (2014). The *Arabidopsis* EDR1 protein kinase negatively regulates the ATL1 E3 ubiquitin ligase to suppress cell death. Plant Cell **26:** 4532–4546.

Shi, H., Shen, Q., Qi, Y., Yan, H., Nie, H., Chen, Y., Zhao, T., Katagiri, F., and Tang, D. (2013). BR-SIGNALING KINASE1 physically associates with FLAGELLIN SENSING2 and regulates plant innate immunity in *Arabidopsis*. Plant Cell **25:** 1143–1157.

Spallek, T., Beck, M., Ben Khaled, S., Salomon, S., Bourdais, G., Schellmann, S., and Robatzek, S. (2013). ESCRT-I mediates FLS2 endosomal sorting and plant immunity. PLoS Genet. **9:** e1004035.

Stein, M., Dittgen, J., Sánchez-Rodríguez, C., Hou, B.-H., Molina, A., Schulze-Lefert, P., Lipka, V., and Somerville, S. (2006). *Arabidopsis* PEN3/PDR8, an ATP binding cassette transporter, contributes to nonhost resistance to inappropriate pathogens that enter by direct penetration. Plant Cell **18:** 731–746.

Tang, D., Ade, J., Frye, C.A., and Innes, R.W. (2005). Regulation of plant defense responses in Arabidopsis by EDR2, a PH and START domain-containing protein. Plant J. **44:** 245–257.

Tang, D., Ade, J., Frye, C.A., and Innes, R.W. (2006). A mutation in the GTP hydrolysis site of Arabidopsis dynamin-related protein 1E confers enhanced cell death in response to powdery mildew infection. Plant J. **47:** 75–84.

Tena, G., Boudsocq, M., and Sheen, J. (2011). Protein kinase signaling networks in plant innate immunity. Curr. Opin. Plant Biol. **14:** 519–529.

Underwood, W., and Somerville, S.C. (2008). Focal accumulation of defences at sites of fungal pathogen attack. J. Exp. Bot. **59:** 3501–3508.

Underwood, W., and Somerville, S.C. (2013). Perception of conserved pathogen elicitors at the plasma membrane leads to relocalization of the Arabidopsis PEN3 transporter. Proc. Natl. Acad. Sci. USA **110:** 12492–12497.

Veronese, P., Nakagami, H., Bluhm, B., Abuqamar, S., Chen, X., Salmeron, J., Dietrich, R.A., Hirt, H., and Mengiste, T. (2006). The membrane-anchored BOTRYTIS-INDUCED KINASE1 plays distinct roles in *Arabidopsis* resistance to necrotrophic and biotrophic pathogens. Plant Cell **18:** 257–273.

Vorwerk, S., Schiff, C., Santamaria, M., Koh, S., Nishimura, M., Vogel, J., Somerville, C., and Somerville, S. (2007). EDR2 negatively regulates salicylic acid-based defenses and cell death during powdery mildew infections of *Arabidopsis thaliana*. BMC Plant Biol. **7:** 35.

Wang, Y., Nishimura, M.T., Zhao, T., and Tang, D. (2011). ATG2, an autophagy-related protein, negatively affects powdery mildew resistance and mildew-induced cell death in Arabidopsis. Plant J. **68:** 74–87.

Wawrzynska, A., Christiansen, K.M., Lan, Y., Rodibaugh, N.L., and Innes, R.W. (2008). Powdery mildew resistance conferred by loss of the ENHANCED DISEASE RESISTANCE1 protein kinase is suppressed by a missense mutation in KEEP ON GOING, a regulator of abscisic acid signaling. Plant Physiol. **148:** 1510–1522.

Wildermuth, M.C., Dewdney, J., Wu, G., and Ausubel, F.M. (2001). Isochorismate synthase is required to synthesize salicylic acid for plant defence. Nature **414:** 562–565.

Xiao, S., Calis, O., Patrick, E., Zhang, G., Charoenwattana, P., Muskett, P., Parker, J.E., and Turner, J.G. (2005). The atypical

resistance gene, RPW8, recruits components of basal defence for powdery mildew resistance in Arabidopsis. Plant J. **42:** 95–110.

Xie, D.-X., Feys, B.F., James, S., Nieto-Rostro, M., and Turner, J.G. (1998). COI1: An Arabidopsis gene required for jasmonate-regulated defense and fertility. Science **280:** 1091–1094.

Yao, C., Wu, Y., Nie, H., and Tang, D. (2012). RPN1a, a 26S proteasome subunit, is required for innate immunity in Arabidopsis. Plant J. **71:** 1015–1028.

Yi, M., and Valent, B. (2013). Communication between filamentous pathogens and plants at the biotrophic interface. Annu. Rev. Phytopathol. **51:** 587–611.

Yoshimoto, K., Jikumaru, Y., Kamiya, Y., Kusano, M., Consonni, C., Panstruga, R., Ohsumi, Y., and Shirasu, K. (2009). Autophagy negatively regulates cell death by controlling NPR1-dependent salicylic acid signaling during senescence and the innate immune response in *Arabidopsis*. Plant Cell **21:** 2914–2927.

Zhang, J., et al. (2007). A *Pseudomonas syringae* effector inactivates MAPKs to suppress PAMP-induced immunity in plants. Cell Host Microbe **1:** 175–185.

Zhao, C., Nie, H., Shen, Q., Zhang, S., Lukowitz, W., and Tang, D. (2014). EDR1 physically interacts with MKK4/MKK5 and negatively regulates a MAP kinase cascade to modulate plant innate immunity. PLoS Genet. **10:** e1004389.

Zipfel, C., Robatzek, S., Navarro, L., Oakeley, E.J., Jones, J.D.G., Felix, G., and Boller, T. (2004). Bacterial disease resistance in Arabidopsis through flagellin perception. Nature **428:** 764–767.